MASTER THESIS

A Non-Hermitian Analysis of Strongly Correlated Quantum Systems

Yuichi Nakamura

Department of Physics,
Graduate School of Science,
The University of Tokyo

4-6-1Komaba, Meguro, Tokyo 153-8505, Japan

January 6, 2005

Abstract

We propose a novel method of calculating the correlation length of strongly correlated quantum systems. The method is to use a non-Hermitian generalization of the quantum systems where the transfer energy of electrons is asymmetric. We show for exactly solvable one-dimensional systems that the non-Hermitian critical point of the ground state, where the energy gap vanishes, is equal to the inverse of the correlation length. We expect that this technique is also applicable to various quantum systems that we cannot solve analytically. We numerically calculate the correlation length of the Hubbard ladder and the $S = 1/2$ antiferromagnetic Heisenberg ladder.

Contents

Chapter 1

Introduction

In the present thesis, we propose a novel method of calculating the correlation length of various quantum systems, particularly the Hubbard model. The Hubbard model is important in discussing properties of strongly correlated electron systems systematically. The one-dimensional Hubbard model is given by the Hamiltonian

$$\mathcal{H} = -t \sum_{i,\sigma} (c^{\dagger}_{i+1,\sigma} c_{i,\sigma} + c^{\dagger}_{i,\sigma} c_{i+1,\sigma}) + U \sum_{i} c^{\dagger}_{i,\uparrow} c_{i,\uparrow} c^{\dagger}_{i,\downarrow} c_{i,\downarrow}, \tag{1.1}$$

where $c^{\dagger}_{i,\sigma}$ and $c_{i,\sigma}$ are the creation and annihilation operators of an electron at site i, respectively. The coefficient t is the nearest-neighbor hopping energy and U is the on-site repulsive Coulomb interaction. Lieb and Wu [1] analytically solved the half-filled one-dimensional Hubbard model of infinite size by the Bethe-ansatz method. They showed that the Mott insulator persists for any finite U. An energy gap due to the charge excitation exists; the gap due to the excitation of a hole of the quasimomentum $\pm\pi$ is often called the Hubbard gap. On the other hand, the energy gap due to the spinon excitation does not exist.

It is a long-standing problem to calculate analytically the correlation function for the one-dimensional Hubbard model, namely, the equal-time one-particle Green's function of the charge excitation; only the asymptotic form has been obtained. Stafford and Millis [2] derived by the Bethe-ansatz method, the analytical expression of the correlation length ξ of the charge excitation at zero temperature in the half-filled case:

$$1/\xi = \frac{4t}{U} \int_{1}^{\infty} \frac{\ln(y + \sqrt{y^2 - 1})}{\cosh(2\pi t y/U)} dy. \tag{1.2}$$

They obtained this expression by considering the size dependence of the Drude weight at zero temperature. Umeno and Shiroishi [3] numerically calculated by the quantum transfer matrix method, the correlation length of the charge excitation at finite temperatures. They confirmed that their numerical data converges to Eq. (1.2) in the zero-temperature limit.

We first show that our method of calculating the correlation length reproduces Eq. (1.2). We then apply it to quantum ladder models. New materials that contain

weakly coupled arrays of metal-oxide ladders are of experimental interest recently. For example, $SrCu_2O_3$ contains two-leg ladders and $Sr_2Cu_3O_5$ contains three-leg ladders [4] with Cu-O-Cu rungs. We can study properties of these materials using the Hubbard ladder models. The two-leg Hubbard ladder has an energy gap due to the charge excitation as well as the spinon excitation. We estimate its correlation length corresponding to the charge gap and the spin gap. The Gutzwiller approximation [5] is often used for strongly correlated electron systems in higher dimensions in order to estimate the correlation function. However, Yokoyama and Shiba [6] pointed out that the Gutzwiller wave function does not yield the Mott insulating phase for any finite U.

Our novel method uses a non-Hermitian generalization of the Hubbard model where the transfer energy of electrons is asymmetric. For example, the non-Hermitian generalization of Eq. (1.1) is

$$\mathcal{H} = -t \sum_{i,\sigma} (e^{g} c^{\dagger}_{i+1,\sigma} c_{i,\sigma} + e^{-g} c^{\dagger}_{i,\sigma} c_{i+1,\sigma}) + U \sum_{i} c^{\dagger}_{i,\uparrow} c_{i,\uparrow} c^{\dagger}_{i,\downarrow} c_{i,\downarrow}, \tag{1.3}$$

where g is the non-Hermiticity parameter. This technique was first introduced by Hatano and Nelson [7], who discussed the localization-delocalization transition of the random Anderson model. They related a non-Hermitian critical point to the inverse localization length. We apply the same technique to the Hubbard model, expecting that the non-Hermitian critical point is related to the inverse correlation length.

Fukui and Kawakami [8] analytically derived the exact solution of the one-dimensional non-Hermitian Hubbard model (1.5) by the Bethe-ansatz method. They obtained the non-Hermitian critical point $g_{\rm c}$ at which the Hubbard gap vanishes. In fact, we confirm that $g_{\rm c}$ is equal to the inverse correlation length of the charge excitation, Eq. (1.2).

We also consider the non-Hermitian generalization of the $S = 1/2$ antiferromagnetic XXZ chain

$$\mathcal{H} = -J \sum_{i=1}^{L} \left[\frac{1}{2} (S^{+}_{i} S^{-}_{i+1} + S^{-}_{i} S^{+}_{i+1}) + \Delta S^{z}_{i} S^{z}_{i+1} \right], \tag{1.4}$$

which has the energy gap due to the spinon excitation for $\Delta < -1$ and $J > 0$. The non-Hermitian XXZ chain was analytically solved by Albertini, Dahmen and Wehefritz [9]. We confirm that the non-Hermitian critical point $g_{\rm c}$ is the inverse correlation length of the spinon excitation.

We thus expect that the present method is applicable to various quantum systems. We define $g_{\rm c}$ for finite systems as the point where the ground-state energy becomes complex. We can calculate the correlation length of the infinite system by extrapolating finite-size data of $g_{\rm c}$. We confirm that this extrapolation works in calculating the correlation length of the one-dimensional Hubbard model, the ferromagnetic Heisenberg chain and the antiferromagnetic XXZ chain. We also discuss

the validity of the extrapolation for various quantum systems, applying it to the Hubbard ladder and the antiferromagnetic Heisenberg ladder.

The present thesis is organized as follows: in Chapter 2, we introduce the non-Hermitian generalization of quantum systems where the transfer energy of electrons is asymmetric. In Chapter 3, we review the Bethe-ansatz solution of the one-dimensional non-Hermitian Hubbard model. We extrapolate the finite-size data of the non-Hermitian critical point g_c to the inverse correlation length of the infinite system. In Chapter 4, we apply the present technique to the Hubbard ladder model. We develop a parallel discussion for the $S = 1/2$ antiferromagnetic XXZ chain in Chapter 5 and for the antiferomagnetic Heisenberg ladder in Chapter 6. In Chapter 7, we summarize our discussions and give prospects of our method.

We propose a novel method of calculating the correlation length of strongly correlated quantum systems. The method is to use a non-Hermitian generalization of the quantum systems where the transfer energy of electrons is asymmetric. This technique was first introduced by Hatano and Nelson[1], who discussed the localization-delocalization transition of the random Anderson model. They related a non-Hermitian critical point to the inverse localization length.

We apply the same technique to strongly correlated quantum systems. We show for exactly solvable one-dimensional systems that the non-Hermitian critical point of the ground state, where the energy gap vanishes, is equal to the inverse of the correlation length. The non-Hermitian Hubbard Hamiltonian in the form

$$\mathcal{H} = -t \sum_{i,\sigma} (e^{g} c^{\dagger}_{i+1,\sigma} c_{i,\sigma} + e^{-g} c^{\dagger}_{i,\sigma} c_{i+1,\sigma}) + U \sum_{i} c^{\dagger}_{i,\uparrow} c_{i,\uparrow} c^{\dagger}_{i,\downarrow} c_{i,\downarrow}, \tag{1.5}$$

eliminates the Hubbard gap as we increase the non-Hermiticity g. The non-Hermitian critical point g_c[2] at which the Hubbard gap vanishes is equal to the inverse correlation length of the charge excitation[3]. The non-Hermitian antiferromagnetic XXZ Hamiltonian in the form

$$\mathcal{H} = -J \sum_{i=1}^{L} \left[\frac{1}{2} (e^{2g} S^{+}_{i} S^{-}_{i+1} + e^{-2g} S^{-}_{i} S^{+}_{i+1}) + \Delta S^{z}_{i} S^{z}_{i+1} \right], \tag{1.6}$$

eliminates the energy gap due to the spin excitation as we increase the non-Hermiticity gand the non-Hermitian critical point g_c[4] at which the energy gap vanishes is equal to the inverse correlation length of the spin excitation[5].

We expect that this technique is applicable to various quantum systems that we cannot solve analytically. We define gcfor finite systems as the point where the ground-state energy becomes complex. We can calculate the correlation length of the infinite system by extrapolating finite-size data of g_c. We show that this extrapolation works well in calculating the correlation length of the one-dimensional Hubbard model and the antiferromagnetic XXZ chain. We relatively accurately estimated the inverse correlation length from the data of g_c for very small systems.

It is a merit of our novel method. We also discuss the validity of the extrapolation for various quantum systems, applying it to the Hubbard ladder and the antiferromagnetic Heisenberg ladder.

[1] N. Hatano and D. R. Nelson, Phys. Rev. Lett. 77(1996) 570; Phys. Rev. B 56(1997) 8651 [2] T. Fukui and N. Kawakami, Phys. Rev. B 58(1998) 16051 [3] C. A. Stafford and A. J. Millis, Phys. Rev. B 48(1993) 1409 [4] G. Albertini, S. R. Dahmen and B. Wehefritz, Nucl. Phys. B 493(1997) 541 [5]R. J. Baxter, Exactly Solved Models in Statistical Mechanics(Academic Press, New York, 1982) p155

Chapter 2

Non-Hermitian generalization of quantum systems

In this chapter, we consider the non-Hermitian generalization of quantum systems by introducing an imaginary vector potential $ig(x)$. The non-Hermitian kinetic energy in the one-dimensional continuous space is given by [7]

$$\mathcal{H}_{\rm k} = \frac{(-i\hbar\nabla + ig(x))^2}{2m}, \tag{2.1}$$

where $g(x)$ is a real scaler. The second-quantized form in the one-dimensional lattice space with a constant imaginary vector potential is given by

$$\mathcal{H}_{\rm k} = -t\sum_{l,\sigma}(e^{g}c^{\dagger}_{l+1,\sigma}c_{l,\sigma} + e^{-g}c^{\dagger}_{l,\sigma}c_{l+1,\sigma}), \tag{2.2}$$

where we set $g(x) = \hbar g$ with g a real constant.

We demonstrate an application of the non-Hermitian generalization (2.2), which was first discussed by Hatano and Nelson [7] for the random Anderson model. We can estimate the localization length only by observing the energy-spectrum flow upon increasing the non-Hermiticity g, that is, without calculating the wave function directly. A one-electron non-Hermitian Anderson model in one dimension is given by

$$\mathcal{H} = -t\sum_{x=-\infty}^{\infty}\left(e^{g}|x+1\rangle\langle x| + e^{-g}|x\rangle\langle x+1|\right) + \sum_{x=-\infty}^{\infty}V_x|x\rangle\langle x|, \tag{2.3}$$

where V_x is a random potential at site x. In solving the non-Hermitian Schrödinger equations

$$\begin{aligned}\mathcal{H}\Psi^R_g(x) &= \varepsilon_g\Psi^R_g(x),\\ \Psi^L_g(x)\mathcal{H} &= \varepsilon_g\Psi^L_g(x),\end{aligned} \tag{2.4}$$

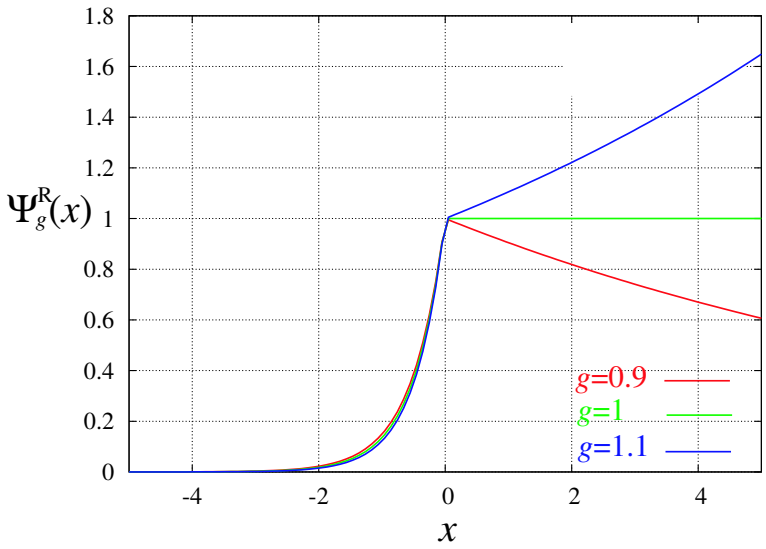

Figure 2.1: The right eigenfunction $\Psi_g^R = e^{gx-|x|}$ for $g = 0.9, 1$ and 1.1. The non-Hermitian critical point is $g_c = 1$ in this case.

we look for the right eigenfunction $\Psi_g^R(x)$ and the left eigenfunction $\Psi_g^L(x)$ in the normalizable functional space. A localized eigenfunction for $g = 0$ is, except for an oscillatory factor, asymptotically given by

$$\Psi_0(x) \sim e^{-\kappa|x|}, \tag{2.5}$$

where κ is the inverse localization length and we set the localization center to $x = 0$ for simplicity. We here introduce the imaginary vector potential $i\hbar g$. We readily see that the right and the left wavefunctions [7]

$$\Psi_g^R(x) = e^{gx}\Psi_0(x), \tag{2.6}$$
$$\Psi_g^L(x) = e^{-gx}\Psi_0(x), \tag{2.7}$$

satisfy Eq. (2.4) with the same eigenvalue as in the Hermitian case, namely $\varepsilon_g = \varepsilon_0$. We refer to Eqs. (2.6) and (2.7) as the imaginary gauge transformation. Equations (2.6) and (2.7) with Eq. (2.5) yield

$$\Psi_g^R(x) \sim e^{gx-\kappa|x|}, \qquad \Psi_g^L(x) \sim e^{-gx-\kappa|x|}, \tag{2.8}$$

which is schematically shown in Fig. 2.1 for $\kappa = 1$. The right and left eigenfunctions are indeed normalizable for $|g| < \kappa$, that is,

$$\Psi_g^R(\pm\infty) \to 0, \qquad \Psi_g^L(\pm\infty) \to 0, \tag{2.9}$$

and hence they can be a solution of Eq. (2.4) in the normalizable functional space.

However, the solution changes dramatically for $|g| > \kappa$. The functions of the forms (2.6) and (2.7) diverge as

$$\Psi_g^R(+\infty) \to \infty, \qquad \Psi_g^L(-\infty) \to \infty, \tag{2.10}$$

and are not normalizable any more. They are no longer the solution in the normalizable functional space. In fact, an extended wavefunction

$$\Psi_g^{R(L)}(x) \sim e^{ikx} \tag{2.11}$$

with an approximate eigenvalue

$$\varepsilon_g \cong \frac{(\hbar k + i\hbar g)^2}{2m}. \tag{2.12}$$

is permitted [7]. Note that ε_g is a complex number depending on g. In numerical calculations, we can reproduce the above for finite systems under the periodic boundary condition:

$$\mathcal{H} = -t \sum_{x=1}^{L} \left(e^g |x+1\rangle\langle x| + e^{-g} |x\rangle\langle x+1| \right) + \sum_{x=1}^{L} V_x |x\rangle\langle x|, \tag{2.13}$$

where the site $L+1$ is identified with the site 1. The spectrum of periodic systems converge to Eq. (2.12) as $L \to \infty$. The functions (2.6) and (2.7) satisfy the periodic boundary condition for $|g| < \kappa$ because of Eq. (2.9) in the large L limit, while they never satisfy the periodic boundary condition for $|g| > \kappa$ because of Eq. (2.10) in the large L limit.

We define the non-Hermitian critical point $g_{\rm c}(L)$ at which the eigenvalues change from real to complex for system size L. We presume that $g_{\rm c}(L)$ converges to the inverse localization length κ for the infinite system as $L \to \infty$. We thus estimate the inverse localization length κ only by observing the spectrum change, not by calculating the wave function directly. It is a merit of the non-Hermitian generalization.

Chapter 3

Non-Hermitian analysis of the 1D Hubbard model

3.1 Non-Hermitian generalization of the Hubbard model

In this section, we consider the non-Hermitian generalization of the Hubbard model. We propose a technique of introducing the non-Hermiticity g in order to eliminate the charge gap and the spin gap separately. The non-Hermiticity g in the form

$$\mathcal{H}_{\rm c}(g) = -t\sum_{l=1}^{L}(e^{g}c_{l+1,\uparrow}^{\dagger}c_{l,\uparrow}+e^{-g}c_{l,\uparrow}^{\dagger}c_{l+1,\uparrow}+e^{g}c_{l+1,\downarrow}^{\dagger}c_{l,\downarrow}+e^{-g}c_{l,\downarrow}^{\dagger}c_{l+1,\downarrow})+U\sum_{l=1}^{L}c_{l,\uparrow}^{\dagger}c_{l,\uparrow}c_{l,\downarrow}^{\dagger}c_{l,\downarrow} \tag{3.1}$$

should eliminate the charge gap, while the one in the form

$$\mathcal{H}_{\rm s}(g) = -t\sum_{l=1}^{L}(e^{g}c_{l+1,\uparrow}^{\dagger}c_{l,\uparrow}+e^{-g}c_{l,\uparrow}^{\dagger}c_{l+1,\uparrow}+e^{-g}c_{l+1,\downarrow}^{\dagger}c_{l,\downarrow}+e^{g}c_{l,\downarrow}^{\dagger}c_{l+1,\downarrow})+U\sum_{l=1}^{L}c_{l,\uparrow}^{\dagger}c_{l,\uparrow}c_{l,\downarrow}^{\dagger}c_{l,\downarrow} \tag{3.2}$$

should eliminate the spin gap. The above idea comes from the first-order perturbation of the Hamiltonians in terms of g. The Hamiltonian (3.1) yields

$$\begin{aligned}\mathcal{H}_{\rm c}(g)-\mathcal{H}_{\rm c}(0) &\cong -gt\sum_{l=1}^{L}(c_{l+1,\uparrow}^{\dagger}c_{l,\uparrow}-c_{l,\uparrow}^{\dagger}c_{l+1,\uparrow}+c_{l+1,\downarrow}^{\dagger}c_{l,\downarrow}-c_{l,\downarrow}^{\dagger}c_{l+1,\downarrow})\\ &= -ig(J_{\uparrow}+J_{\downarrow}),\end{aligned} \tag{3.3}$$

and the Hamiltonian (3.2) yields

$$\begin{aligned}\mathcal{H}_{\rm s}(g)-\mathcal{H}_{\rm s}(0) &\cong -gt\sum_{l=1}^{L}(c_{l+1,\uparrow}^{\dagger}c_{l,\uparrow}-c_{l,\uparrow}^{\dagger}c_{l+1,\uparrow}-c_{l+1,\downarrow}^{\dagger}c_{l,\downarrow}+c_{l,\downarrow}^{\dagger}c_{l+1,\downarrow})\\ &= -ig(J_{\uparrow}-J_{\downarrow}),\end{aligned} \tag{3.4}$$

where $J_\sigma(\sigma =\uparrow,\downarrow)$ is the paramagnetic current operator defined by

$$J_\sigma \equiv -it\sum_{l=1}^{L}(c_{l+1,\sigma}^\dagger c_{l,\sigma} - c_{l,\sigma}^\dagger c_{l+1,\sigma}). \tag{3.5}$$

Hence $J_\uparrow + J_\downarrow$ is the charge current operator and $J_\uparrow - J_\downarrow$ is the spin current operator. We expect to calculate the correlation length due to the charge and the spinon excitations separately by applying this technique. It is of great interest to calculate the correlation length of quantum systems with both the charge gap and the spin gap, for example, the Hubbard ladders [10] and the Kondo lattice models [11].

3.2 Exact analysis of the non-Hermitian Hubbard model

3.2.1 Exact solution of the Bethe-ansatz equation

In this section, we review the analytic solution [8] of the non-Hermitian Hamiltonian (3.1) by the Bethe-ansatz method and confirm that the non-Hermitian critical point is equal to Eq. (1.2) .

We make the following ansatz for the eigenfunction Ψ_g, considering the imaginary gauge transformation (2.6) [8]:

$$\begin{aligned}\Psi_g(x_1,x_2,\ldots,x_M|x_{M+1},\ldots,x_N) &= \exp\left(g\sum_{j=1}^{N}x_j\right)\Psi_0(x_1,x_2,\ldots,x_M|x_{M+1},\ldots,x_N)\\ &= \sum_P [Q,P]\exp(i\sum_{j=1}^{N}(k_{P_j}-ig)x_{Q_j}),\end{aligned} \tag{3.6}$$

where the wave function Ψ_0 is the Bethe-ansatz wave function in the Hermitian case $g = 0$:

$$\Psi_0(x_1,x_2,\ldots,x_M|x_{M+1},\ldots,x_N) = \sum_P [Q,P]\exp(i\sum_{j=1}^{N}k_{P_j}x_{Q_j}), \tag{3.7}$$

and L, M and N are the number of the lattice, the number of the down spins and the number of the electrons, respectively. We put the down spins at $x_1, x_2, \ldots, x_M$ and the up spins at $x_{M+1}, \ldots, x_N$. The symbols $P = (P_1, P_2, \ldots, P_N)$ and $Q = (Q_1, Q_2, \ldots, Q_N)$ are two permutations of the set $(1, 2, \ldots, N)$ with $1 \le x_{Q_1} \le x_{Q_2} \le \cdots \le x_{Q_N} \le L$. The symbol $[Q, P]$ is a set of $N! \times N!$ coefficients depending on the two permutations P and Q. The quasimomenta $k_1, k_2, \ldots, k_N$ are unequal to each other for the ground state [12].

The non-Hermitian Bethe-ansatz equation is then given by [8]

$$\exp(iLk_j + gL) = \prod_{\beta=1}^{M} \frac{\sin k_j - \Lambda_\beta + iU/4t}{\sin k_j - \Lambda_\beta - iU/4t} \qquad (j = 1, \ldots, N),$$
$$\prod_{j=1}^{N} \frac{\sin k_j - \Lambda_\alpha + iU/4t}{\sin k_j - \Lambda_\alpha - iU/4t} = -\prod_{\beta=1}^{M} \frac{\Lambda_\alpha - \Lambda_\beta - iU/4t}{\Lambda_\alpha - \Lambda_\beta + iU/4t} \qquad (\alpha = 1, \ldots, M). \tag{3.8}$$

By taking the logarithm of Eq. (3.8), we have

$$k_j L - igL = 2\pi I_j - 2\sum_{\beta=1}^{M} \arctan \frac{\sin k_j - \lambda_\beta}{U/4t},$$
$$-2\sum_{j=1}^{N} \arctan \frac{\sin k_j - \lambda_\alpha}{U/4t} = 2\pi J_\alpha + 2\sum_{\beta=1}^{M} \arctan \frac{\lambda_\alpha - \lambda_\beta}{U/2t}, \tag{3.9}$$

where the quantum numbers I_j and J_α for the ground state are given by

$$I_j = \frac{N-1}{2}, \frac{N-3}{2}, \ldots, -\frac{N-1}{2},$$
$$J_\alpha = \frac{M-1}{2}, \frac{M-3}{2}, \ldots, -\frac{M-1}{2}. \tag{3.10}$$

We here consider the half-filled case where $L = N$ and $M = N/2$. By solving Eq. (3.9) numerically, we obtain the distributions of the rapidities k and λ in the complex plain for a finite system. Figure 3.1 shows the distribution of k for the ground state of the infinite system. We define $\mathcal{C}$ as the curve where the rapidity k lies. The end points of the curves $\mathcal{C}$ are denoted by $\pm\pi + i\kappa$. The distribution of λ is on the real axis from $-\infty$ to ∞. We rewrite Eq. (3.9) in the form of Fredholm-type integral equations:

$$k - ig = 2\pi z_{\mathcal{C}}(k) - \int_{-\infty}^{\infty} 2\arctan \frac{\sin k - \lambda}{U/4t} \sigma(\lambda) d\lambda,$$
$$\int_{\mathcal{C}} 2\arctan \frac{\lambda - \sin k}{U/4t} \rho(k) dk = 2\pi z_{\mathcal{S}}(\lambda) + \int_{-\infty}^{\infty} 2\arctan \frac{\lambda - \lambda'}{U/2t} \sigma(\lambda') d\lambda', \tag{3.11}$$

where $z_{\mathcal{C}}(k_j) = I_j/L$, $z_{\mathcal{S}}(\lambda) = J_\alpha/L$, $\rho(k) \equiv z'_{\mathcal{C}}(k)$ and $\sigma(\lambda) \equiv z'_{\mathcal{S}}(\lambda)$. By differentiating Eq. (3.11) with respect to k and λ, we have

$$\rho(k) = \frac{1}{2\pi} + \frac{\cos k}{\pi} \int_{-\infty}^{\infty} \frac{U/4t}{(U/4t)^2 + (\lambda - \sin k)^2} \sigma(\lambda) d\lambda,$$
$$\sigma(\lambda) = \frac{1}{\pi} \int_{\mathcal{C}} \frac{U/4t}{(U/4t)^2 + (\lambda - \sin k)^2} \rho(k) dk - \frac{1}{\pi} \int_{-\infty}^{\infty} \frac{U/2t}{(U/2t)^2 + (\lambda - \lambda')^2} \sigma(\lambda') d\lambda'. \tag{3.12}$$

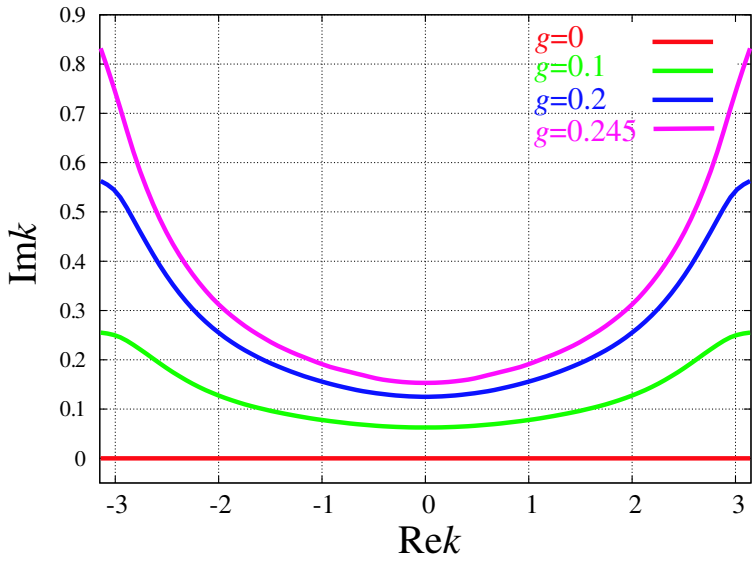

Figure 3.1: The distribution of the charge rapidity k for the infinite system with $U/t = 4$. We plot the data for $g = 0, 0.1, 0.2$ and 0.245. The end points are $\pm\pi + 0.0881i$ as $g \to g_c = 0.246$.

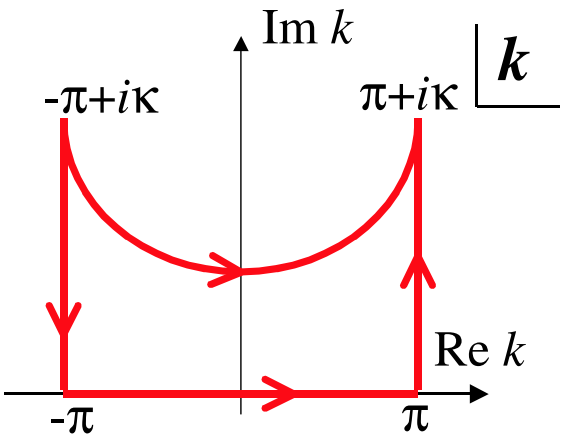

Figure 3.2: The loop $C_{\mathcal{C}}$ in the complex k plain.

We here consider the loops $C_{\mathcal{C}}$ in the k plain as shown in Fig 3.2. The poles of the integrand $(U/4t)/[(U/4t)^2 + (\lambda - \sin k)^2]$ in the k plain get closest to the real axis for $\lambda = 0$,

$$k_n = \pm i\mathrm{arcsinh}(U/4t) + n\pi \qquad (n = 0, \pm 1). \tag{3.13}$$

As long as there are no poles in $C_{\mathcal{C}}$, we can modify the integral contour as [8]

$$\int_{\mathcal{C}} = \int_{-\pi+i\kappa}^{-\pi} + \int_{-\pi}^{\pi} + \int_{\pi}^{\pi+i\kappa}. \tag{3.14}$$

Thus we rewrite Eq. (3.12) in the forms

$$\rho(k) = \frac{1}{2\pi} + \frac{\cos k}{\pi}\int_{-\infty}^{\infty} \frac{U/4t}{(U/4t)^2 + (\lambda - \sin k)^2}\sigma(\lambda)d\lambda, \tag{3.15}$$

$$\begin{aligned}\sigma(\lambda) = {} & \frac{1}{\pi}\int_{-\pi}^{\pi} \frac{U/4t}{(U/4t)^2 + (\lambda - \sin k)^2}\rho(k)dk + \frac{1}{\pi}\int_{\pi}^{\pi+i\kappa} \frac{U/4t}{(U/4t)^2 + (\lambda - \sin k)^2}\rho(k)dk \\ & + \frac{1}{\pi}\int_{-\pi+i\kappa}^{-\pi} \frac{U/4t}{(U/4t)^2 + (\lambda - \sin k)^2}\rho(k)dk - \frac{1}{\pi}\int_{-\infty}^{\infty} \frac{U/2t}{(U/2t)^2 + (\lambda - \lambda')^2}\sigma(\lambda')d\lambda'.\end{aligned} \tag{3.16}$$

Since the integrand is a periodic function with respect to k, we readily see

$$\frac{1}{\pi}\int_{\pi}^{\pi+i\kappa} \frac{U/4t}{(U/4t)^2 + (\lambda - \sin k)^2}\rho(k)dk + \frac{1}{\pi}\int_{-\pi+i\kappa}^{-\pi} \frac{U/4t}{(U/4t)^2 + (\lambda - \sin k)^2}\rho(k)dk = 0. \tag{3.17}$$

Hence we have

$$\sigma(\lambda) = \frac{1}{\pi}\int_{-\pi}^{\pi} \frac{U/4t}{(U/4t)^2 + (\lambda - \sin k)^2}\rho(k)dk - \frac{1}{\pi}\int_{-\infty}^{\infty} \frac{U/2t}{(U/2t)^2 + (\lambda - \lambda')^2}\sigma(\lambda')d\lambda'. \tag{3.18}$$

Equations (3.15) and (3.18) are the same as in the Hermitian case reviewed in Appendix A.2. The solution is

$$\rho(k) = \frac{1}{2\pi} + \frac{\cos k}{\pi}\int_0^\infty \frac{\cos(\omega \sin k) J_0(\omega)}{1+\exp(\omega U/2t)} d\omega,$$
$$\sigma(\lambda) = \frac{1}{2\pi}\int_0^\infty \mathrm{sech}\left(\frac{U}{4t}\omega\right)\cos(\lambda\omega) J_0(\omega) d\omega, \tag{3.19}$$

where $J_0(\omega)$ is the Bessel function of the first kind.

As long as there are no poles in $C_{\mathcal{C}}$, the ground state energy per site is

$$\begin{aligned} E_{\mathrm{gs}} &= -2t\int_{\mathcal{C}} \cos k\rho(k) dk \\ &= -2t\int_{-\pi}^{\pi} \cos k\rho(k) dk - 2t\int_{-\pi}^{-\pi+i\kappa} \cos k\rho(k) dk - 2t\int_{\pi}^{\pi+i\kappa} \cos k\rho(k) dk. \end{aligned} \tag{3.20}$$

Since $\cos k\rho(k)$ is a periodic function with respect to k, we have

$$-2t\int_{-\pi}^{-\pi+i\kappa} \cos k\rho(k) dk - 2t\int_{\pi}^{\pi+i\kappa} \cos k\rho(k) dk = 0. \tag{3.21}$$

Hence E_{gs} is given by

$$E_{\mathrm{gs}} = -2t\int_{-\pi}^{\pi} \cos k\rho(k) dk = -4t\int_0^\infty \frac{J_0(\omega)J_1(\omega)}{\omega(1+\exp(\omega U/2t))} d\omega. \tag{3.22}$$

The ground state energy does not depend on g.

3.2.2 What happens to the system at g_{c}?

In this section, we calculate the non-Hermitian critical point g_{c} analytically and observe what happens to the system at g_{c}. We define g_{c} as the point at which the end points of the curve $\mathcal{C}$ reaches the poles in Eq. (3.13), $k_1 = i\mathrm{arcsinh}(U/4t) + \pi$. We also show that the Hubbard gap vanishes at this point.

By considering Eq. (3.11), the critical point g_{c} is given by

$$\begin{aligned} g_{\mathrm{c}} &= \lim_{\Lambda\to\infty}\lim_{k\to k_1 - i0}\left(2\pi i z_{\mathcal{C}}(k) - ik - i\int_{-\Lambda}^{\Lambda} 2\arctan\frac{\sin k - \lambda}{U/4t}\sigma(\lambda)d\lambda\right) \\ &= \lim_{\Lambda\to\infty}\lim_{\kappa\to\kappa_{\mathrm{c}}-0}\left(\kappa + 2i\int_{-\Lambda}^{\Lambda}\arctan\frac{\lambda + i\sinh\kappa}{U/4t}\sigma(\lambda)d\lambda\right) \\ &= \lim_{\Lambda\to\infty}\left[\mathrm{arcsinh}(U/4t) + 2i\int_{-\Lambda}^{\Lambda}\arctan\frac{\lambda + iU/4t}{U/4t}\sigma(\lambda)d\lambda\right] \\ &= \lim_{\Lambda\to\infty}\left[\mathrm{arcsinh}(U/4t) + \frac{i}{\pi}\int_{-\Lambda}^{\Lambda} d\lambda \arctan\frac{\lambda + iU/4t}{U/4t}\int_0^\infty \frac{\cos(\omega\lambda)J_0(\omega)}{\cosh((U/4t)\omega)}d\omega\right], \end{aligned} \tag{3.23}$$

where $\kappa_{\rm c} \equiv \mathrm{arcsinh}(U/4t)$ and we used

$$z_{\mathcal{C}}(k_{\pm 1}) = \pm\frac{(L-1)/2}{L} \to \pm\frac{1}{2} \qquad \text{as} \quad L \to \infty. \tag{3.24}$$

Using the variable transformation

$$\theta = \arctan(\lambda/(U/4t) + i) \tag{3.25}$$

with

$$\tan\theta_1 = -\frac{\Lambda}{U/4t} + i, \quad \tan\theta_2 = \frac{\Lambda}{U/4t} + i, \tag{3.26}$$

we have

$$\begin{aligned} g_{\rm c} &= \lim_{\Lambda\to\infty}\left[\mathrm{arcsinh}(U/4t) + \frac{i}{\pi}\int_{\theta_1}^{\theta_2}\frac{(U/4t)\theta}{\cos^2\theta}\left[\int_0^{\infty}\frac{\cos((U/4t)\omega\tan\theta - i(U/4t)\omega)J_0(\omega)d\omega}{\cosh((U/4t)\omega)}\right]d\theta\right] \\ &= \lim_{\Lambda\to\infty}\left[\mathrm{arcsinh}(U/4t) + \frac{i}{\pi}\int_0^{\infty}\frac{(U/4t)J_0(\omega)d\omega}{\cosh((U/4t)\omega)}\left\{\underbrace{\left[\frac{\sin((U/4t)\omega\tan\theta - i(U/4t)\omega)}{(U/4t)\omega}\theta\right]_{\theta_1}^{\theta_2}}_{I_1}\right.\right. \\ &\qquad \left.\left. - \underbrace{\int_{\theta_1}^{\theta_2}\frac{\sin((U/4t)\omega\tan\theta - i(U/4t)\omega)}{(U/4t)\omega}d\theta}_{I_2}\right\}\right]. \end{aligned} \tag{3.27}$$

We rewrite I_1 in the form

$$\begin{aligned} I_1 =& \frac{1}{(U/4t)\omega}\left\{\theta_2\sin((U/4t)\omega\tan\theta_2 - i(U/4t)\omega) - \theta_1\sin((U/4t)\omega\tan\theta_1 - i(U/4t)\omega)\right\} \\ =& \frac{1}{(U/4t)\omega}(\theta_1+\theta_2)\sin(\omega\Lambda), \end{aligned} \tag{3.28}$$

where the coefficients θ_1 and θ_2 for $\Lambda \gg 1$ are in the form

$$\theta_1 = -\frac{\pi}{2} - \delta_1, \qquad \theta_2 = \frac{\pi}{2} - \delta_2 \tag{3.29}$$

with $|\delta_1|, |\delta_2| \ll 1$. Because of

$$\tan\theta_1 = -\frac{1}{\tan\delta_1} \simeq -\frac{1}{\delta_1}, \qquad \tan\theta_2 = -\frac{1}{\tan\delta_2} \simeq -\frac{1}{\delta_2}, \tag{3.30}$$

we have

$$\begin{aligned} I_1 &= \frac{1}{(U/4t)\omega}(-\delta_1 - \delta_2)\sin(\omega\Lambda) \\ &= \frac{1}{(U/4t)\omega}\left(-\frac{U/4t}{i(U/4t)-\Lambda} - \frac{U/4t}{i(U/4t)+\Lambda}\right)\sin(\omega\Lambda) \\ &= \frac{2i(U/4t)}{\omega((U/4t)^2+\Lambda^2)}\sin(\omega\Lambda) \\ &\xrightarrow{\Lambda\to\infty} 0. \end{aligned} \tag{3.31}$$

Next we calculate I_2. By using the variable transformation $x = \tan\theta - i$, we have

$$\begin{aligned} I_2 &= \lim_{\Lambda\to\infty}\int_{-\Lambda/(U/4t)}^{\Lambda/(U/4t)} \frac{\sin((U/4t)\omega x)}{(U/4t)\omega}\frac{dx}{1+(x+i)^2} \\ &= \int_{-\infty}^{\infty}\frac{\sin((U/4t)\omega x)}{(U/4t)\omega(x^2+2ix)}dx = \frac{\pi}{2i(U/4t)\omega}(1-e^{-2\omega(U/4t)}). \end{aligned} \tag{3.32}$$

We thus arrive at [8]

$$\begin{aligned} g_{\rm c} =& \text{arcsinh}(U/4t) - \frac{i}{\pi}\int_0^\infty \frac{(U/4t)J_0(\omega)}{\cosh((U/4t)\omega)}\frac{\pi}{2i(U/4t)\omega}(1-e^{-2\omega(U/4t)})d\omega \\ =& \text{arcsinh}(U/4t) - 2\int_0^\infty \frac{J_0(\omega)\sinh((U/4t)\omega)}{\omega(1+e^{2(U/4t)\omega})}d\omega \qquad (3.33) \\ =& \frac{4t}{U}\int_1^\infty \frac{\ln(y+\sqrt{y^2-1})}{\cosh(2\pi t y/U)}dy \qquad (3.34) \end{aligned}$$

Note that $g_{\rm c}$ in Eq. (3.34) is equal to the inverse correlation length (1.2) due to the charge excitation, obtained by Stafford and Millis [2]. Figure 3.3 shows the U/t dependence of $g_{\rm c} = 1/\xi$. For large U, we have $g_{\rm c} \sim \text{arcsinh}(U/4t)$ by neglecting the second term of Eq. (3.33).

Next we show that the Hubbard gap vanishes at $g_{\rm c}$. The Hubbard gap is given by (see Appendix A.3)

$$\Delta E(k_h) = U + 4t\left[\cos k_h + \int_{-\infty}^{\infty} d\omega \frac{\exp(i\omega\sin k_h)J_1(\omega)}{\omega(1+e^{U|\omega|/2t})}\right], \tag{3.35}$$

where k_h is the rapidity of the hole. The lowest charge excitation at $k_h = \pm\pi + i\kappa$ gives the Hubbard gap as a function of κ in the form

$$\begin{aligned} \Delta E(\kappa) =& U + 4t\left[-\cosh\kappa + \int_{-\infty}^{\infty} d\omega \frac{\exp(\omega\sinh\kappa)J_1(\omega)}{\omega(1+e^{U|\omega|/2t})}\right] \\ =& U - 4t\cosh\kappa - 4t\sum_{n=1}^{\infty}(-1)^n[\sqrt{1+(2(U/4t)n-\sinh\kappa)^2} \\ &+ \sqrt{1+(2(U/4t)n+\sinh\kappa)^2} - 4(U/4t)n]. \end{aligned} \tag{3.36}$$

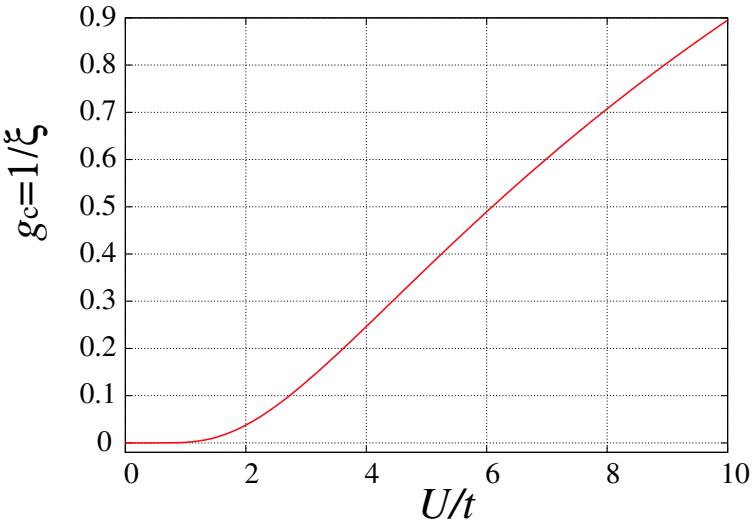

Figure 3.3: The U/t dependence of $g_c = \xi^{-1}$.

At $\kappa = \kappa_c$, we have

$$\begin{aligned} E(\kappa_c) =& U - 4t\sqrt{1+(U/4t)^2} - 4t\sum_{n=1}^{\infty}(-1)^n[\sqrt{1+(U/4t)^2(2n-1)^2} \\ & - (U/4t)(2n-1) + \sqrt{1+(U/4t)^2(2n+1)^2} - (U/4t)(2n+1)] \\ =& U - 4t\sqrt{1+(U/4t)^2} - 4t\Big[(-1)\{\sqrt{1+(U/4t)^2} - (U/4t)\} \\ & + \lim_{n\to\infty}(-1)^n\{\sqrt{1+(U/4t)^2(2n+1)^2} - (U/4t)(2n+1)\}\Big] \\ =& 0, \end{aligned} \tag{3.37}$$

since

$$\lim_{n\to\infty}(-1)^n\{\sqrt{1+(U/4t)^2(2n+1)^2} - (U/4t)(2n+1)\} = 0.$$

To summarize, the Hubbard gap vanishes at $\kappa = \kappa_c$, or $g = g_c$. Figure 3.4 shows how the Hubbard gap vanishes as we increase the non-Hermiticity g for $U/t = 4$.

3.3 Numerical analysis of the non-Hermitian Hubbard model

3.3.1 Spectrum flow of the non-Hermitian Hubbard model

In the previous section, we confirmed that the non-Hermitian critical point g_c, where the Hubbard gap vanishes, is equal to the inverse correlation length of the charge

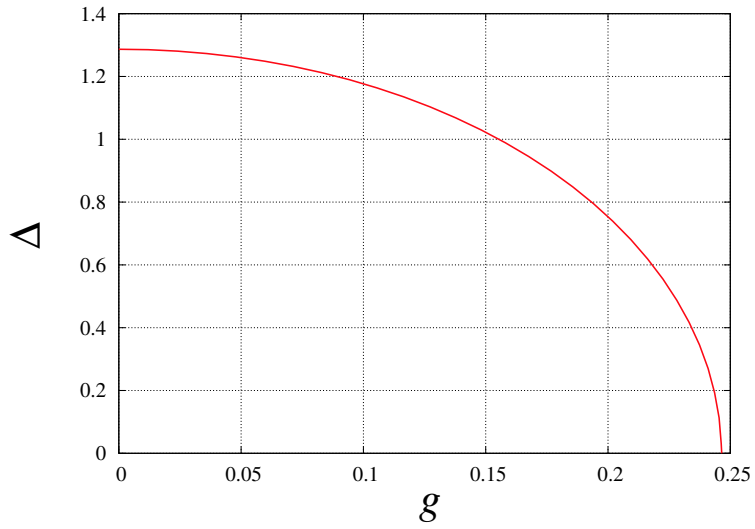

Figure 3.4: The g dependence of the Hubbard gap Δ for $U/t = 4$.

excitation for the infinite Hubbard chain. We here show that we can estimate the correlation length of the infinite system by extrapolating finite-size data of g_c. This is our novel method of calculating the correlation length. In this section, we calculate g_c for finite non-Hermitian Hubbard chains. We work in the subspace where the numbers of the up spins and the down spins are the same.

We first use the non-Hermiticity g in the form (3.1) in order to eliminate the charge gap. All eigenvalues are real for $g = 0$. Upon increasing g, a pair of eigenvalues move on the real axis and spread into the complex plain when g is over a value. Figure 3.5 (a) shows the spectrum flow for $L = 4$ around the ground state. The eigenvalues of the ground state and the third excited state move toward each other on the real axis and spread into the complex plain as soon as the two eigenvalues collide. We here define the non-Hermitian critical point g_c as the point where the ground-state eigenvalue becomes complex. The eigenvalues of the first and the second excited states scarcely move. The ground-state energy does not change for $g < g_c$ for the infinite system. The movement of the ground-state energy is presumably a finite-size effect.

On the other hand, Fig. 3.5 (b) shows the spectrum flow for $L = 4$ around the ground state when we use g in the form (3.2) in order to eliminate the spin gap. The eigenvalues of the first and the second excited states move toward each other, while the eigenvalues of the ground state and the third excited state scarcely move. We presume that the energy gap between the ground state and the third excited state is caused by the charge excitation and that between the first and the second excited states is caused by the spinon excitation. This behavior corresponds to the charge-spin separation of one-dimensional quantum systems in the low energy region. We

(a)

(b)

Figure 3.5: The spectrum flow of the real part of the eigenvalues around the ground state for $L = 4$ with $U/t = 2$ as we introduce the non-Hermiticity g in order to vanish (a) the charge gap and (b) the spin gap.

estimated the non-Hermitian critical points, $g_{\rm c}^{(\rm c)}$ from Fig. 3.5 (a) and $g_{\rm c}^{(\rm s)}$ from Fig. 3.5 (b), respectively for $L = 4$.

Figure 3.6 shows the spectrum flow in a higher energy region. The states at A, B and C have the degeneracy 2, 4 and 2, respectively for $g = 0$. The energy gap between the states A and B and that between the states B and C vanish when we increase g in the form (3.1) as well as (3.2). This behavior implies that the excitations are caused by mixture of charge and spin in higher energy regions.

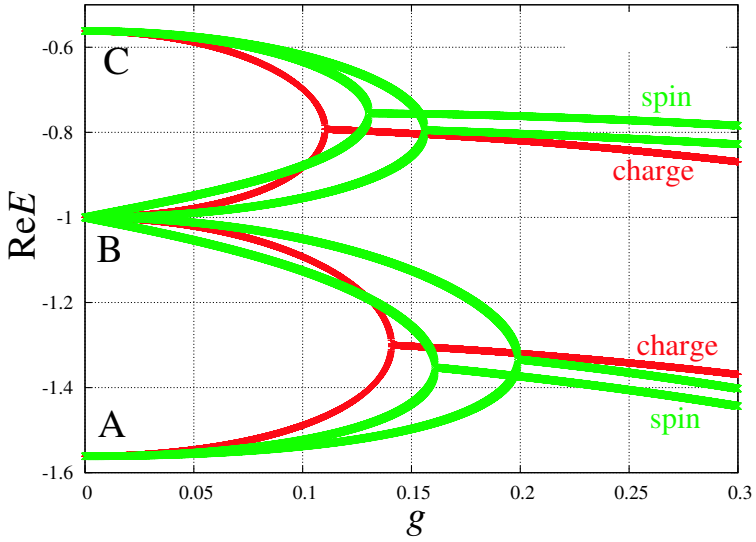

Figure 3.6: The spectrum flow of the real part of the eigenvalues in a higher energy region for $L = 4$ with $U/t = 2$ as we introduce the non-Hermiticity g in order to vanish the energy gap due to the charge excitation (the red line) and the spinon excitation (the green line).

3.3.2 Numerical calculation of g_c

We next calculate $g_c^{(c)}$ and $g_c^{(s)}$ for $L = 4, 6$ and 8, and extrapolate them to $g_c^{(c)}$ and $g_c^{(s)}$ for the infinite system by considering finite-size corrections. Figure 3.7 shows the $1/L$ plot of $g_c^{(c)}$ and $g_c^{(s)}$. We here assumed the following finite-size correction to g_c:

$$g_c(L) = g_c + a/L + \mathrm{O}(1/L^2). \tag{3.38}$$

We fit the data to a linear function of $1/L$ by the least-squares method. The final estimates of $g_c^{(c)}$ and $g_c^{(s)}$ are 0.438 and -0.028, while the Bethe-ansatz method yields 0.382 and 0, respectively. Our estimates are consistent with the exact values. It is quite remarkable to obtain such good estimates from data for such small L.

(a)

(b)

Figure 3.7: (a) The $1/L$ plot of $g_{\rm c}^{(\rm c)}$ and (b) the $1/L$ plot of $g_{\rm c}^{(\rm s)}$ for $L = 4, 6$ and 8. We set $U/t = 2$.

Chapter 4

Numerical calculation of the correlation length of the Hubbard ladder model

In the previous chapter, we discussed the possibility of extrapolating the finite-size data of $g_{\rm c}$ to the inverse correlation length of the infinite system. We confirmed that our technique works for the one-dimensional Hubbard model. We show in the present chapter that this technique is also applicable to other quantum systems. We estimate the correlation length of the two-leg Hubbard ladder. Ground-state properties of the two-leg Hubbard ladder were investigated by Noack, White and Scalapino [10]. They claimed that the charge gap as well as the spin gap exist. We here try to estimate the correlation length $\xi_{\rm c}$ due to the charge gap using the form (3.1) and $\xi_{\rm s}$ due to the spin gap using the form (3.2). The two-leg Hubbard ladder is given by

$$\mathcal{H} = \mathcal{H}_{\rm leg1} + \mathcal{H}_{\rm leg2} + \mathcal{H}_{\rm rung}, \tag{4.1}$$

where $\mathcal{H}_{{\rm leg}j} \quad (j = 1, 2)$ and $\mathcal{H}_{\rm rung}$ are

$$\mathcal{H}_{{\rm leg}j} = -t \sum_{i,\sigma}^{L} (c^{\dagger}_{i+1,j,\sigma} c_{i,j,\sigma} + c^{\dagger}_{i,j,\sigma} c_{i+1,j,\sigma}) + U \sum_{i}^{L} c^{\dagger}_{i,j,\uparrow} c_{i,j,\uparrow} c^{\dagger}_{i,j,\downarrow} c_{i,j,\downarrow} \quad (j = 1, 2),$$

$$\mathcal{H}_{\rm rung} = -t_{\perp} \sum_{i,\sigma}^{L} (c^{\dagger}_{i,1,\sigma} c_{i,2,\sigma} + c^{\dagger}_{i,2,\sigma} c_{i,1,\sigma}), \tag{4.2}$$

with t the intra-chain hopping energy and $t_{\perp}$ the inter-chain hopping energy. We apply the periodic boundary conditions. As in Eqs. (3.1) and (3.2), the non-Hermiticity g in the form

$$\mathcal{H}^{\rm (c)}_{{\rm leg}j}(g) = -t \sum_{i,\sigma}^{L} (e^{g} c^{\dagger}_{i+1,j,\sigma} c_{i,j,\sigma} + e^{-g} c^{\dagger}_{i,j,\sigma} c_{i+1,j,\sigma}) + U \sum_{i}^{L} c^{\dagger}_{i,j,\uparrow} c_{i,j,\uparrow} c^{\dagger}_{i,j,\downarrow} c_{i,j,\downarrow} \tag{4.3}$$

should eliminate the charge gap, while the one in the form

$$\mathcal{H}^{(\mathrm{s})}_{\mathrm{leg}j}(g) = -t\sum_{i}^{L}(e^{g}c^{\dagger}_{i+1,j,\uparrow}c_{i,j,\uparrow} + e^{-g}c^{\dagger}_{i,j,\uparrow}c_{i+1,j,\uparrow}$$
$$+ e^{-g}c^{\dagger}_{i+1,j,\downarrow}c_{i,j,\downarrow} + e^{g}c^{\dagger}_{i,j,\downarrow}c_{i+1,j,\downarrow}) + U\sum_{i}^{L}c^{\dagger}_{i,j,\uparrow}c_{i,j,\uparrow}c^{\dagger}_{i,j,\downarrow}c_{i,j,\downarrow} \tag{4.4}$$

should eliminate the spin gap.

We estimate $g_{\mathrm{c}}^{(\mathrm{c})}$ and $g_{\mathrm{c}}^{(\mathrm{s})}$, where the ground-state energy becomes complex, for the Hubbard ladder of finite size. Figure 4 shows the spectrum flow of the real part of eigenvalues around the ground state for $L = 4$ as we increase g in the forms (3.1) and (3.2) for $U/t = 1$ and $t_{\perp}/t = 2$. The energy gap between the ground state A and the excited state B vanishes in both cases. We suppose that the excitation between the state A and the state B are caused by mixture of charge and spin and this result is not consistent with a ground-state property that Noack *et al.* argued [10]: the energy gap due to the charge excitation and that due to the spinon excitation exist. We expect that we can calculate the non-Hermitian critical points $g_{\mathrm{c}}^{(\mathrm{c})}$ and $g_{\mathrm{c}}^{(\mathrm{s})}$ separately for larger systems $L = 6, 8$. The dimensionality of the Hamiltonian, however, are 8.5×10^6 for $L = 6$ and 1.7×10^8 for $L = 8$, respectively. We have the limitation of diagonalizing the Hamiltonians by means of LAPACK, which consumes $\mathrm{O}(N^2)$ memory. Quite recently, Hatano [13] developed an $\mathrm{O}(N)$ algorithm of calculating the energy spectrum of huge non-Hermitian matrices by means of both the Lanczos method and the biconjugate gradient method. We try to calculate $g_{\mathrm{c}}^{(\mathrm{c})}$ and $g_{\mathrm{c}}^{(\mathrm{s})}$ for $L = 6, 8$, and to extrapolate them to the correlation length ξ_{c} due to the charge gap and ξ_{s} due to the spin gap of the infinite system.

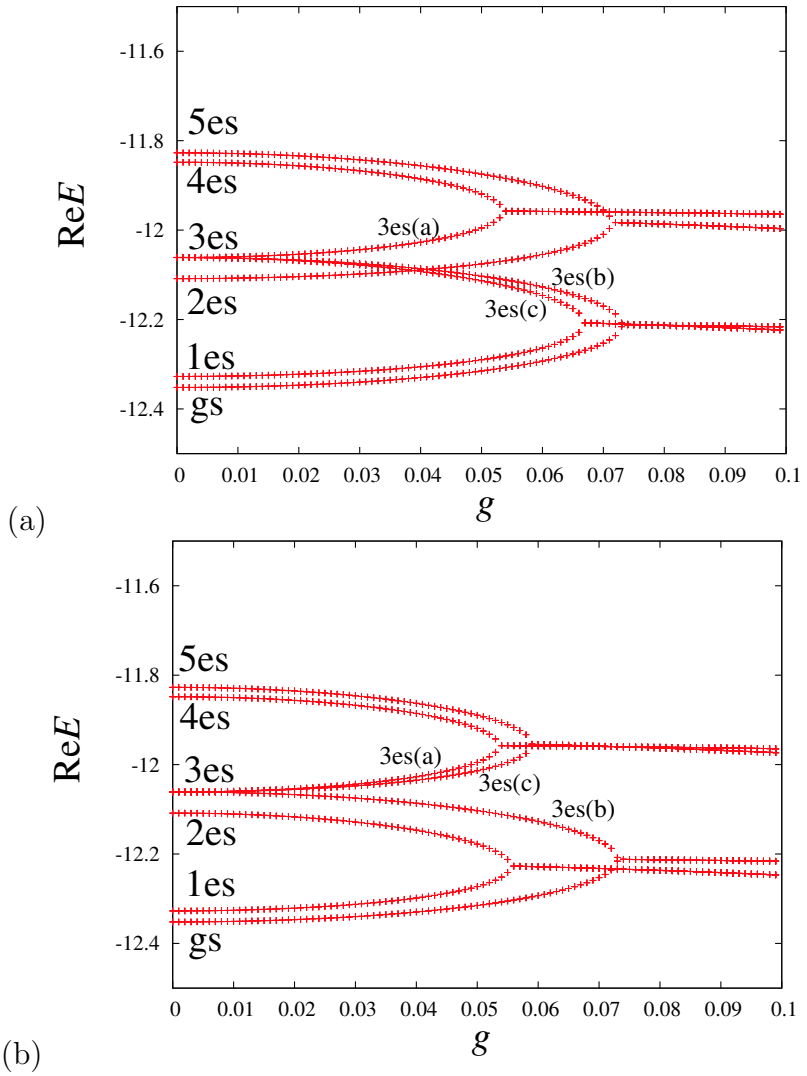

Figure 4.1: The spectrum flow of the real part of eigenvalues around the ground state for $L = 4$ with $U/t = 1$ and $t_\perp/t = 2$ as we introduce g (a) in the form Eq. (3.1) and (b) in the form Eq. (3.2).

Chapter 5

Non-Hermitian analysis of the 1D XXZ chain

5.1 Non-Hermitian generalization of the XXZ chain

In this chapter, we make a non-Hermitian analysis of the $S = 1/2$ antiferromagnetic XXZ chain, which has an energy gap due to the spinon excitation. The non-Hermitian XXZ chain was exactly solved by the Bethe-ansatz method. We see that the non-Hermitian critical point $g_{\rm c}$ at which the energy gap vanishes is equal to the inverse correlation length of the spinon excitation.

The XXZ chain is given by

$$\mathcal{H} = -J \sum_{i=1}^{L} \left[\frac{1}{2} \left(S_i^- S_{i+1}^+ + S_i^+ S_{i+1}^- \right) + \Delta S_i^z S_{i+1}^z \right] \tag{5.1}$$

for $\Delta < -1$ and $J > 0$, where $S_i^{\pm} = \frac{1}{2}(\sigma_i^x \pm i\sigma_i^y)$ and $S_i^z = \frac{1}{2}\sigma^z$ with the Pauli spin operators $\sigma^x, \sigma^y, \sigma^z$. The number of the lattice L is even. The spin-spin correlation length of the XYZ chain for the arbitrary J_x, J_y and J_z was obtained by Johnson, Krinsky and McCoy [14] by the Bethe-ansatz method. The correlation length of the spinon excitation for the XXZ chain is given by [15]

$$\frac{1}{\xi} = \frac{\gamma}{2} + \sum_{n=1}^{\infty} \frac{(-1)^n}{n} \tanh(n\gamma), \tag{5.2}$$

where $\gamma = \operatorname{arccosh}(-\Delta)$.

We now consider a non-Hermitian generalization of Eq. (5.1):

$$\mathcal{H} = -J \sum_{i=1}^{L} \left[\frac{1}{2} \left(e^{2g} S_i^- S_{i+1}^+ + e^{-2g} S_i^+ S_{i+1}^- \right) + \Delta S_i^z S_{i+1}^z \right]. \tag{5.3}$$

The reason for the factors $e^{\pm 2g}$ is as follows. We start from the non-Hermitian Hubbard model in order to vanish the spin gap, Eq. (3.2):

$$\mathcal{H} = \mathcal{H}_t + \mathcal{H}_U \tag{5.4}$$

where

$$\begin{aligned}
\mathcal{H}_t &= -t \sum_{i=1}^{L} (e^{g} c_{i+1,\uparrow}^{\dagger} c_{i,\uparrow} + e^{-g} c_{i,\uparrow}^{\dagger} c_{i+1,\uparrow} + e^{-g} c_{i+1,\downarrow}^{\dagger} c_{i,\downarrow} + e^{g} c_{i,\downarrow}^{\dagger} c_{i+1,\downarrow}), \\
\mathcal{H}_U &= U \sum_{i}^{L} c_{i,\uparrow}^{\dagger} c_{i,\uparrow} c_{i,\downarrow}^{\dagger} c_{i,\downarrow}.
\end{aligned} \tag{5.5}$$

The Heisenberg model is derived from the half-filled Hubbard model in the large U limit, by considering the perturbation expansion with respect to the kinetic energy around the degenerate ground state. The ground state of $\mathcal{H}_U$ in the half-filled case has a ${}_L C_{L/2}$-fold degeneracy; all of the ground states $|\psi_n^{\rm gs}\rangle$ are composed of the states with no double occupancy. Since the first-order perturbation energy vanishes, the degeneracy is lifted in the second order. Hence the effective Hamiltonian $\mathcal{H}_{\rm eff}$ is given by

$$\mathcal{H}_{\rm eff} = \sum_{n} \frac{\mathcal{H}_t |\psi_n^{\rm es}\rangle\langle\psi_n^{\rm es}| \mathcal{H}_t}{\mathcal{H}_U - E_{\rm es}(n)} = -\sum_{n} \frac{\mathcal{H}_t |\psi_n^{\rm es}\rangle\langle\psi_n^{\rm es}| \mathcal{H}_t}{U}, \tag{5.6}$$

where $|\psi_n^{\rm es}\rangle$ with the eigenvalue $E_{\rm es}(n)$ denotes a first-excited state with one double occupancy and one empty site. The Hilbert space of $\mathcal{H}_{\rm eff}$ is spanned by $|\psi_n^{\rm gs}\rangle$. Hence

we can write down the effective Hamiltonian $\mathcal{H}_{\rm eff}$ as

$$\begin{aligned}
\mathcal{H}_{\rm eff} =& -\frac{t^2}{U}\sum_{i=1}^{L}(e^{g}c_{i,\downarrow}^{\dagger}c_{i+1,\downarrow}e^{g}c_{i+1,\uparrow}^{\dagger}c_{i,\uparrow}+e^{-g}c_{i,\uparrow}^{\dagger}c_{i+1,\uparrow}e^{-g}c_{i+1,\downarrow}^{\dagger}c_{i,\downarrow}\\
&+e^{-g}c_{i+1,\downarrow}^{\dagger}c_{i,\downarrow}e^{-g}c_{i,\uparrow}^{\dagger}c_{i+1,\uparrow}+e^{g}c_{i+1,\uparrow}^{\dagger}c_{i,\uparrow}e^{g}c_{i,\downarrow}^{\dagger}c_{i+1,\downarrow})\\
&-\frac{t^2}{U}\sum_{i=1}^{L}(e^{-g}c_{i,\uparrow}^{\dagger}c_{i+1,\uparrow}e^{g}c_{i+1,\uparrow}^{\dagger}c_{i,\uparrow}+e^{g}c_{i+1,\uparrow}^{\dagger}c_{i,\uparrow}e^{-g}c_{i,\uparrow}^{\dagger}c_{i+1,\uparrow}\\
&+e^{g}c_{i,\downarrow}^{\dagger}c_{i+1,\downarrow}e^{-g}c_{i+1,\downarrow}^{\dagger}c_{i,\downarrow}+e^{-g}c_{i+1,\downarrow}^{\dagger}c_{i,\downarrow}e^{g}c_{i,\downarrow}^{\dagger}c_{i+1,\downarrow})\\
=&\frac{2t^2}{U}\sum_{i=1}^{L}(e^{2g}c_{i,\downarrow}^{\dagger}c_{i,\uparrow}c_{i+1,\uparrow}^{\dagger}c_{i+1,\downarrow}+e^{-2g}c_{i,\uparrow}^{\dagger}c_{i,\downarrow}c_{i+1,\downarrow}^{\dagger}c_{i+1,\uparrow})\\
&-\frac{t^2}{U}\sum_{i=1}^{L}[c_{i,\uparrow}^{\dagger}c_{i,\uparrow}(1-c_{i+1,\uparrow}^{\dagger}c_{i+1,\uparrow})+(1-c_{i,\uparrow}^{\dagger}c_{i,\uparrow})c_{i+1,\uparrow}^{\dagger}c_{i+1,\uparrow}\\
&+c_{i,\downarrow}^{\dagger}c_{i,\downarrow}(1-c_{i+1,\downarrow}^{\dagger}c_{i+1,\downarrow})+(1-c_{i,\downarrow}^{\dagger}c_{i,\downarrow})c_{i+1,\downarrow}^{\dagger}c_{i+1,\downarrow}]\\
=&\frac{2t^2}{U}\sum_{i=1}^{L}[e^{2g}c_{i,\downarrow}^{\dagger}c_{i,\uparrow}c_{i+1,\uparrow}^{\dagger}c_{i+1,\downarrow}+e^{-2g}c_{i,\uparrow}^{\dagger}c_{i,\downarrow}c_{i+1,\downarrow}^{\dagger}c_{i+1,\uparrow}]\\
&+\frac{t^2}{U}\sum_{i=1}^{L}[2n_{i,\uparrow}n_{i+1,\uparrow}+2n_{i,\downarrow}n_{i+1,\downarrow}-2],
\end{aligned}\tag{5.7}$$

where we used the fact that all $|\psi_n^{\rm gs}\rangle$ satisfy

$$n_{i,\uparrow}+n_{i,\downarrow}=1.$$

By using the transformations

$$S_i^{+}=c_{i,\uparrow}^{\dagger}c_{i,\downarrow},\quad S_i^{-}=c_{i,\downarrow}^{\dagger}c_{i,\uparrow},\quad S_i^{z}=\frac{1}{2}(n_{i,\uparrow}-n_{i,\downarrow}),$$

we arrive at

$$\mathcal{H}_{\rm eff}=\frac{4t^2}{U}\sum_{i=1}^{L}\left[\frac{1}{2}\left(e^{2g}S_i^{-}S_{i+1}^{+}+e^{-2g}S_i^{+}S_{i+1}^{-}\right)+S_i^{z}S_{i+1}^{z}-\frac{1}{4}\right],\tag{5.8}$$

where we used

$$\begin{aligned}
&2n_{i,\uparrow}n_{i+1,\uparrow}+2n_{i,\downarrow}n_{i+1,\downarrow}=n_{i,\uparrow}n_{i+1,\uparrow}+n_{i,\uparrow}(1-n_{i+1,\downarrow})+n_{i,\downarrow}n_{i+1,\downarrow}+n_{i,\downarrow}(1-n_{i+1,\uparrow})\\
&=(n_{i,\uparrow}-n_{i,\downarrow})(n_{i+1,\uparrow}-n_{i+1,\downarrow})+1=4S_i^{z}S_{i+1}^{z}+1.
\end{aligned}$$

Identifying $J\equiv -4t^2/U$, we have Eq. (5.3) for $\Delta=-1$.

5.2 Exact analysis of the non-Hermitian XXZ chain

The non-Hermitian XXZ chain (5.3) was exactly solved by Albertini, Dahmen and Wehefritz [9] by the Bethe-ansatz method. In the present section, we point out that the non-Hermitian critical point g_c, where the energy gap vanishes, is equal to the inverse correlation length of the spinon excitation, Eq. (5.2).

We now consider the half-filled case, where $\sum_{i=1}^{L} S_i^z = 0$ with L sites, M up spins and M down spins ($M \equiv L/2$). We define the the vacuum state $|\mathrm{vac}\rangle$ as the state where all spins are up. An eigenfunction with M down spins is given by

$$\Psi = \sum_{(x_1,x_2,\ldots,x_M)} \psi_g(x_1, x_2, \ldots, x_M) S_{x_1}^- S_{x_2}^- \ldots S_{x_M}^- |\mathrm{vac}\rangle, \tag{5.9}$$

where we put down spins at $x_1, x_2, \ldots, x_M$ ($1 \le x_1 < x_2 < \cdots < x_M \le L$). We make the following ansatz for the wave function ψ_g [9]:

$$\begin{aligned}\psi_g(x_1, x_2, \ldots, x_M) =& \exp\left(2g \sum_{j=1}^{M} x_j\right) \psi_0(x_1, x_2, \ldots, x_M) \\ =& \sum_P [Q, P] \exp(i \sum_{j=1}^{M} (k_{P_j} - 2ig) x_{Q_j}).\end{aligned} \tag{5.10}$$

The wave function ψ_0 is the Bethe-ansatz wave function in the Hermitian case $g = 0$:

$$\psi_0(x_1, x_2, \ldots, x_M) = \sum_P [Q, P] \exp(i \sum_{j=1}^{M} k_{P_j} x_{Q_j}), \tag{5.11}$$

where the symbols $P = (P_1, P_2, \ldots, P_M)$ and $Q = (Q_1, Q_2, \ldots, Q_M)$ are two permutations of the set $(1, 2, \ldots, M)$ with $1 \le x_{Q_1} \le x_{Q_2} \le \cdots \le x_{Q_M} \le L$. The symbol $[Q, P]$ is a set of $M! \times M!$ coefficients depending on the two permutations P and Q. The quasimomenta $k_1, k_2, \ldots, k_M$ are unequal to each other for the ground state.

We obtain the following Bethe-ansatz equations for $1 \le j \le M$ [9]:

$$\exp(ik_j L + 2gL) = (-1)^{M-1} \prod_{j \ne l}^{M} \frac{\exp[i(k_j + k_l)] + 1 - 2\Delta \exp(ik_j)}{\exp[i(k_j + k_l)] + 1 - 2\Delta \exp(ik_l)}. \tag{5.12}$$

We here introduce a new rapidity parameter λ_j:

$$\exp(ik_j) = -\frac{\sin[\gamma(\lambda_j + i)/2]}{\sin[\gamma(\lambda_j - i)/2]}.$$

Equation (5.12) then becomes

$$\left[\frac{\sin\frac{\gamma}{2}(\lambda_j + i)}{\sin\frac{\gamma}{2}(\lambda_j - i)}\right]^L e^{2gL} = \prod_{j \ne l}^{M} \frac{\sin\frac{\gamma}{2}(\lambda_j - \lambda_l + 2i)}{\sin\frac{\gamma}{2}(\lambda_j - \lambda_l - 2i)}. \tag{5.13}$$

By taking the logarithm of Eq. (5.13), we have

$$2L \arctan\left[\frac{\tan(\gamma\lambda_j/2)}{\tanh(\gamma/2)}\right] = 2\pi I_j + 2igL + 2\sum_{i=1}^{M} \arctan\left[\frac{\tan[\gamma(\lambda_j-\lambda_i)/2]}{\tanh(\gamma)}\right], \quad (5.14)$$

where the quantum number I_j for the ground state is given by

$$I_j = \frac{L/2-1}{2}, \frac{L/2-3}{2}, \ldots, -\frac{L/2-1}{2}. \quad (5.15)$$

The summation in Eq. (5.14) becomes an integral in the limit $L \to \infty$ as

$$2\underbrace{\arctan\left[\frac{\tan(\gamma\lambda/2)}{\tanh(\gamma/2)}\right]}_{\theta_1(\lambda)} = 2\pi z_s(\lambda) + 2ig + 2\int_{\mathcal{S}} \underbrace{\arctan\left[\frac{\tan[\gamma(\lambda-\Lambda)/2]}{\tanh(\gamma)}\right]}_{\theta_2(\lambda-\Lambda)} \sigma(\Lambda)d\Lambda, \quad (5.16)$$

where $z_s(\lambda_j) \equiv I_j/L$, $\sigma(\lambda_j) \equiv z_s'(\lambda_j)$ and $\mathcal{S}$ is the curve in the complex plain on which the rapidity lies as shown in Fig. 5.1. We restrict ourselves to the region $-\pi/\gamma \leq \mathrm{Re}\lambda \leq \pi/\gamma$, since $\theta_1(\lambda)$ in the Eq. (5.16) is a function of the periodicity $2\pi/\gamma$. We have the end points of $\mathcal{S}$ denoted by $\pm\pi/\gamma + i\beta$. The distribution function $\sigma(\lambda)$ satisfies the following integral equation by differentiating Eq. (5.16) with respect to λ:

$$\frac{\gamma \sinh\gamma}{\cosh\gamma - \cos\gamma\lambda} = 2\pi\sigma(\lambda) + \int_{\mathcal{S}} \frac{\gamma\sinh(2\gamma)}{\cosh(2\gamma) - \cos\{\gamma(\lambda-\Lambda)\}}\sigma(\Lambda)d\Lambda. \quad (5.17)$$

The poles of the integrand in Eq. (5.17)

$$\frac{\gamma\sinh(2\gamma)}{\cosh(2\gamma) - \cos\{\gamma(\lambda-\Lambda)\}}$$

in the λ plain are $\lambda - \Lambda = \pm 2i$. They never appear in the loop $C_{\mathcal{S}}$ as shown in Fig. 5.2 as long as $-1 < \mathrm{Im}\lambda < 1$ and $-1 < \mathrm{Im}\Lambda < 1$. When the imaginary part of the end points of the curve $\mathcal{S}$ reaches the points $\beta = 1$ as we increase the non-Hermiticity g, we expect that the system changes dramatically, that is, the energy gap due to the spinon excitation vanishes [9]. We define this critical point as g_{c}.

Let us obtain g_{c}. We can modify the integral contour as long as $g < g_{\mathrm{c}}$ in the form

$$\int_{\mathcal{S}} = \int_{-\pi/\gamma+i\beta}^{-\pi/\gamma} + \int_{-\pi/\gamma}^{\pi/\gamma} + \int_{\pi/\gamma}^{\pi/\gamma+i\beta}. \quad (5.18)$$

We obtain the solution $\sigma(\Lambda)$ by taking the Fourier transformation of $\sigma(\Lambda)$:

$$\sigma(\lambda) = \sum_{n=-\infty}^{n=\infty} \frac{e^{-in\gamma\lambda}}{2\cosh(n\gamma)}. \quad (5.19)$$

We consider the following expansion of $\theta_1(\lambda)$ and $\theta_2(\lambda)$ in Eq. (5.16) in order to make the discussion easy:

$$\theta_1(\lambda) = \gamma\lambda + i\sum_{n\neq 0}\frac{\exp(-in\gamma\lambda - \gamma|n|)}{n},$$
$$\theta_2(\lambda) = \gamma\lambda + i\sum_{n\neq 0}\frac{\exp(-in\gamma\lambda - 2\gamma|n|)}{n}. \tag{5.20}$$

We substitute Eqs. (5.19) and (5.20) into Eq. (5.16) and we have

$$2g = 2\pi i z_{\mathcal{S}}(\lambda) - i\frac{\gamma\lambda}{2} + \sum_{n\neq 0}\frac{e^{-in\gamma\lambda}}{2n\cosh(n\gamma)} + \frac{\gamma\beta}{2} + \sum_{n\neq 0}(-1)^n\frac{e^{n\gamma\beta}}{2n\cosh(n\gamma)}. \tag{5.21}$$

By substituting $\lambda = \pm\pi/\gamma + i\beta$ into Eq. (5.21) we obtain $g(\beta)$ as a function of β in the form

$$\begin{aligned}2g(\beta) =& 2\pi i z_{\mathcal{S}}(\pm\pi/\gamma + i\beta) - i\frac{\gamma}{2}\left(\pm\frac{\pi}{\gamma} + i\beta\right) + \frac{\gamma\beta}{2} + 2\sum_{n=1}^{\infty}\frac{(-1)^n\sinh(n\gamma\beta)}{n\cosh(n\gamma)}\\ =& \gamma\beta + 2\sum_{n=1}^{\infty}\frac{(-1)^n\sinh(n\gamma\beta)}{n\cosh(n\gamma)},\end{aligned} \tag{5.22}$$

since

$$z_{\mathcal{S}}(\pm\pi/\gamma + i\beta) = \frac{\pm(L/2-1)/2}{L} \to \pm\frac{1}{4} \tag{5.23}$$

as $L \to \infty$. Hence we obtain $g_{\rm c}$ by substituting $\beta = 1$:

$$g_{\rm c} = \frac{\gamma}{2} + \sum_{n=1}^{\infty}\frac{(-1)^n\tanh(n\gamma)}{n}. \tag{5.24}$$

The non-Hermitian critical point $g_{\rm c}$ is equal to the inverse spin-spin correlation length Eq. (5.2). The γ dependence of $g_{\rm c} = \xi^{-1}$ is plotted in Fig. 5.3.

5.3 Numerical analysis of the non-Hermitian Heisenberg model

In this section, we numerically calculate $g_{\rm c}$ of the Heisenberg model of finite size and extrapolate the data to the correlation length of the spinon excitation. We investigate the ferromagnetic XXX model ($\Delta = 1$) and the antiferromagnetic XXZ model ($\Delta < -1$). Figure 5.4 shows the spectrum flow around the ground state of the XXX model ($L = 8$) as we introduce the non-Hermiticity g for $\Delta = -4$. We note that a pair of the first and the second excited states undergoes the real-complex

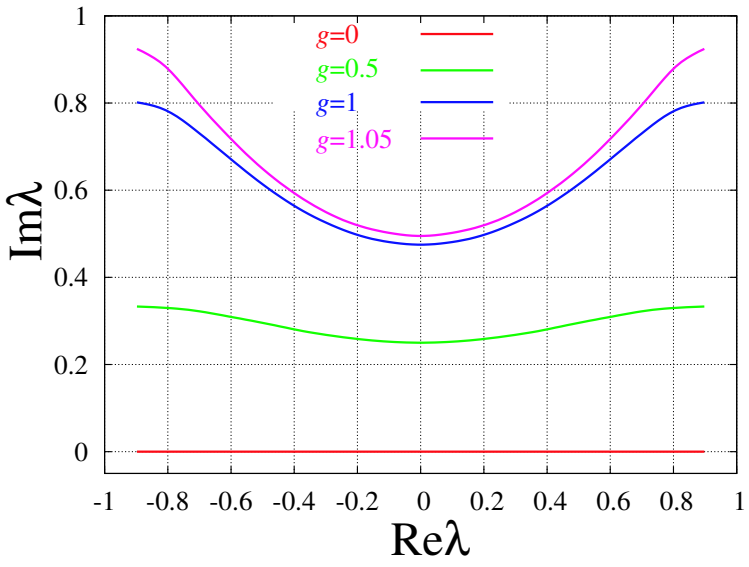

Figure 5.1: The distribution of the spin rapidity λ for the infinite system with $\gamma = 3.5$. In this case, the non-Hermitian critical point g_c is 1.05867.

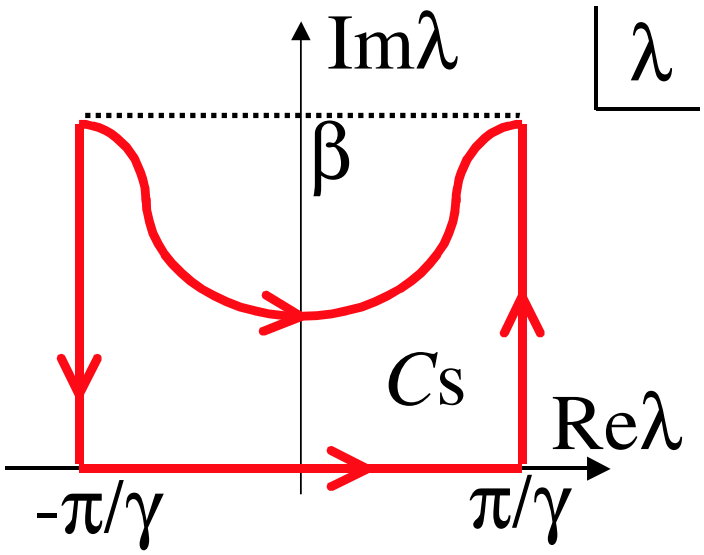

Figure 5.2: The loop C_S in the complex λ plain.

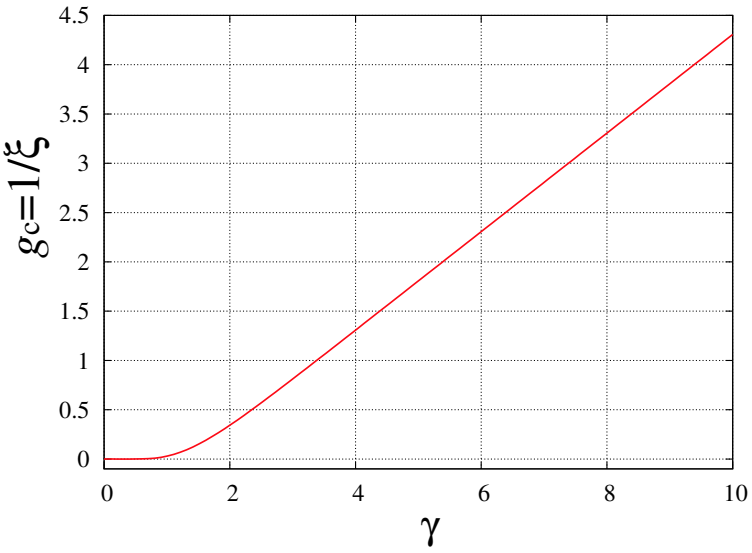

Figure 5.3: The γ dependence of $g_c = \xi^{-1}$.

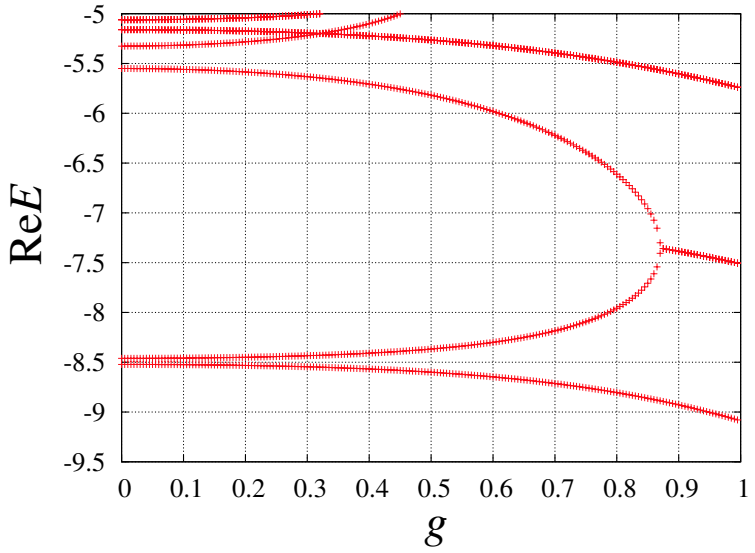

Figure 5.4: The spectrum flow of the XXZ model for $L = 8$ with $\Delta = -4$.

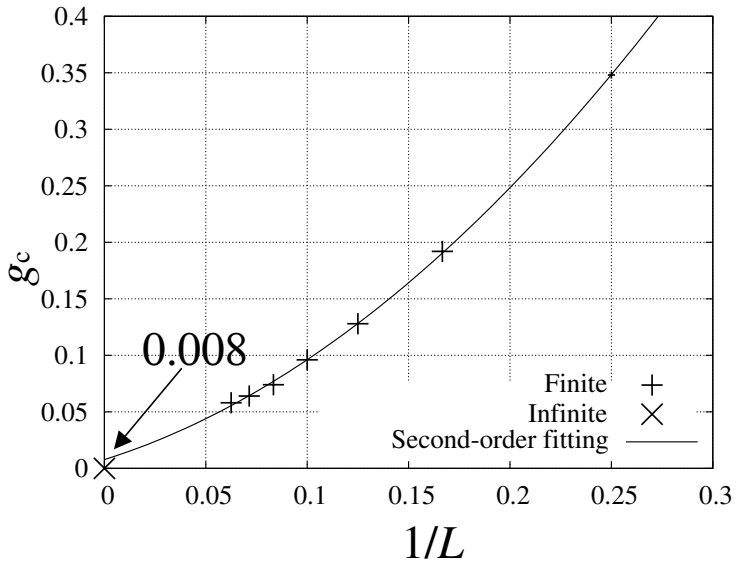

Figure 5.5: The finite-size plot of g_c for the XXX model.

transition and we regard this as the non-Hermitian critical point g_c for a finite size. We here consider the following finite-size correction as

$$g_c(L) = g_c(L = \infty) + f(1/L) \tag{5.25}$$

and fit the data for $L = 4, 6, \ldots, 14, 16$. Figure 5.5 shows the finite-size plot of g_c for the XXX model. The finite-size data approaches zero, consistent with the fact that the spinon excitation from the ground state is gapless. Figure 5.6 shows the finite-size plot of g_c for the XXZ model with $\Delta = -4$. The non-Hermitian critical point $g_c(\infty)$ calculated analytically is 0.772. In both cases, we can extrapolate the finite-size data to g_c of the infinite system. Unfortunately, we cannot derive the expression of $f(1/L)$ and cannot calculate g_c more accurately for now.

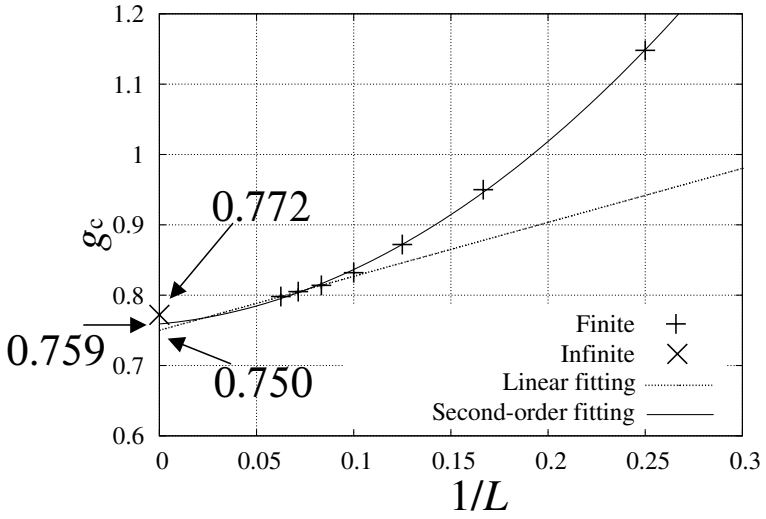

Figure 5.6: The finite-size plot of $g_{\rm c}$ for the XXZ model with $\Delta = -4$.

Chapter 6

Numerical calculation of the correlation length of the Heisenberg ladder

In this chapter, we calculate the correlation length of the spinon excitation of the Heisenberg two-leg ladder. The ladders with even numbers of legs have a finite energy gap by the spinon excitation, while those with odd numbers of legs have no energy gap [16]. The inverse correlation length should be finite in the former case, while zero in the latter case. We here estimate the correlation length of the spinon excitation numerically.

The non-Hermitian $S = 1/2$ Heisenberg two-leg ladder is

$$\mathcal{H} = \mathcal{H}_{\text{leg1}} + \mathcal{H}_{\text{leg2}} + \mathcal{H}_{\text{rung}} \tag{6.1}$$

$$\mathcal{H}_{\text{leg}j} = J \sum_{i=1}^{L} \left[\frac{1}{2}(e^{2g} S^+_{i+1,j} S^-_{i,j} + e^{-2g} S^+_{i,j} S^-_{i+1,j}) + S^z_{i,j} S^z_{i+1,j} \right] \quad (j = 1, 2) \tag{6.2}$$

$$\mathcal{H}_{\text{rung}} = J_\perp \sum_{i=1}^{L} \left[\frac{1}{2}(S^+_{i,1} S^-_{i,2} + S^+_{i,2} S^-_{i,1}) + S^z_{i,1} S^z_{i,2} \right] \tag{6.3}$$

where $J > 0$ and $J_\perp > 0$ in the antiferromagnetic case. We require periodic boundary conditions.

We calculate the finite-size data of g_{c} for $L = 4, 6, 8$ and extrapolate them to g_{c} of the infinite system. Figure 6.1 shows the spectrum flow around the ground state for $L = 4$ with $J_\perp/J = 4.0$. The energy gap between the ground state and the fourth ground state vanishes at $g = g_{\text{c}}$. Figure 6.2 shows the $1/L$ plot of g_{c} for $J_\perp/J = 4$. We here assume the finite-size correction to g_{c} as

$$g_{\text{c}}(L) = g_{\text{c}} + a/L + \text{O}(1/L^2). \tag{6.4}$$

The extrapolated estimated from the finite-size data is 0.089. This result shows that the spin gap exists for the two-leg ladder model. In order to estimate g_{c} more

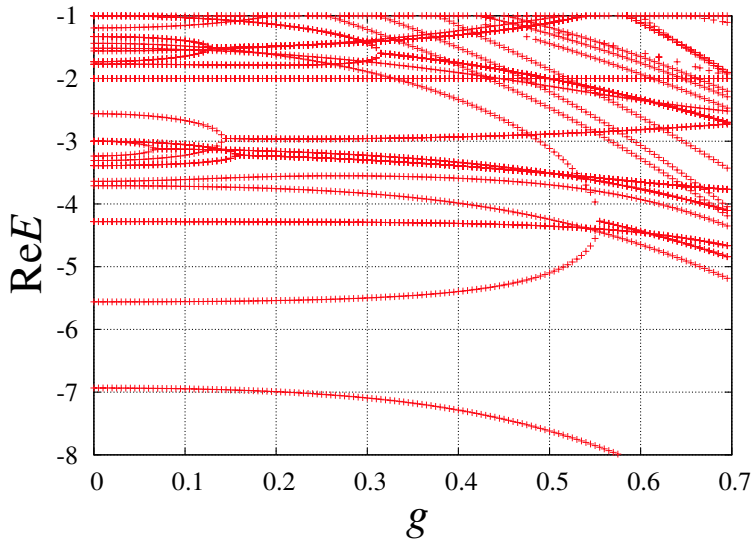

Figure 6.1: The spectrum flow of the real part of the eigenvalues around the ground state for $L = 4$ with $J_\perp/J = 4$.

accurately, we try to calculate $g_c(L)$ for larger sizes by applying the O(N) algorithm of calculating the energy spectrum [13].

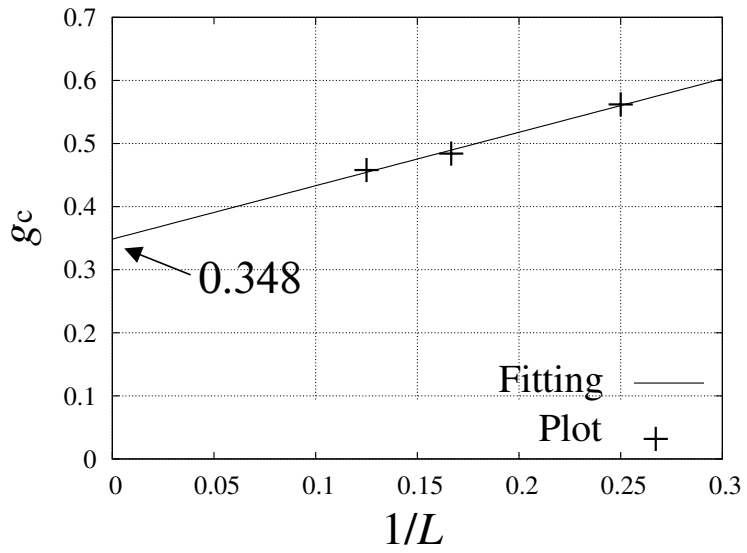

Figure 6.2: The $1/L$ plot of g_c for the $L = 4, 6$ and $L = 8$ with $J_\perp/J = 4$.

Chapter 7

Summary and discussions

We proposed a novel method of calculating the correlation length due to the charge gap and the spin gap of various strongly correlated quantum systems. We confirmed that the non-Hermitian critical point g_c where the energy gap vanishes is equal to the inverse correlation length of the exactly solvable Hubbard model and the XXZ model in one dimension. These length scales never emerge in the *quasimomenta* of the ground state of the Bethe-ansatz method, because all of the quasimomenta are real. However, we expect that the *momenta* of the wave function of the Mott insulator contain complex numbers and that the imaginary part of the momenta corresponds to the inverse correlation length analogously to the discussion of the random Anderson model.

In the numerical study, we extrapolate the finite-size data of g_c to the inverse correlation length of the infinite system. We confirmed that it is applicable to the Hubbard, the Heisenberg and the XXZ model in one dimension. We also apply it to the two-leg Hubbard ladder and the antiferromagnetic two-leg Heisenberg ladder. We obtained the non-Hermitian critical points g_c of the Hubbard ladder for $L = 4$ and that of the Heisenberg ladder for L =4, 6 and 8 by diagonalizing the non-Hermitian matrices numerically. It is a merit of our method that we can obtain a good estimate of g_c for infinite size from the data of g_c for much smaller size.

We are interested in computing g_c for larger systems to extrapolate g_c of the infinite system more accurately. However, we have a bleak prospect for calculating g_c by means of LAPACK, which consumes $\mathrm{O}(N^2)$ memory. Hatano developed an $\mathrm{O}(N)$ algorithm of calculating the energy spectrum of huge non-Hermitian matrices. He relates the eigenvalues of the matrices to the points where the norm of the Green's function diverges [13]. We try to calculating g_c for the Hubbard ladder and the Heisenberg ladder for larger systems by means of the $\mathrm{O}(N)$ algorithm .

Acknowledgement

The author would like to thank Associate Professor Naomichi Hatano for his valuable suggestions and discussions.

Appendix A

Bethe-ansatz method for the 1D Hubbard model

A.1 The Bethe-ansatz method

We can solve a few one-dimensional quantum systems exactly by the Bethe-ansatz method. This method was first introduced by H. Bethe [17] in 1930s to discuss the spin-wave theory of the one-dimensional ferromagnetic Heisenberg model. We regard models that satisfy the Yang-Baxter relation as the exactly solvable models. The exactly solvable models are, for example, the Hubbard model, the Heisenberg model, the Anderson model [18] and so on. The knowledge from the exact solution of the one-dimensional electron systems is important in order to discuss properties of the low-dimensional electron systems.

Lieb and Wu [1] obtained the exact solution of the one-dimensional Hubbard model

$$\mathcal{H} = -t \sum_{i=1,\sigma}^{L} (c_{i+1,\sigma}^{\dagger} c_{i,\sigma} + c_{i,\sigma}^{\dagger} c_{i+1,\sigma}) + U \sum_{i=1}^{L} c_{i,\uparrow}^{\dagger} c_{i,\uparrow} c_{i,\downarrow}^{\dagger} c_{i,\downarrow}, \tag{A.1}$$

by the Bethe-ansatz method. Here $c_{i,\sigma}^{\dagger}$ and $c_{i,\sigma}$ are the creation and annihilation operator of an electron at site i. The coefficient t is the nearest-neighbor hopping energy, U is the on-site repulsive Coulomb interaction and L is the number of the lattice. Then we prepare four states for each site, that are the vacuum state $|\mathrm{vac}\rangle$, the up-spin state $c_{i,\uparrow}^{\dagger}|\mathrm{vac}\rangle$, the down-spin state $c_{i,\downarrow}^{\dagger}|\mathrm{vac}\rangle$ and the full state $c_{i,\uparrow}^{\dagger} c_{i,\downarrow}^{\dagger}|\mathrm{vac}\rangle$. We prepare the subspace where the numbers of the up spins and the down spins are fixed in order to reduce the dimension of the Hilbert space. We assume that the number of the up spins is

$$\sum_{i=1}^{L} c_{i,\uparrow}^{\dagger} c_{i,\uparrow} = N - M \tag{A.2}$$

and the number of the down spins is

$$\sum_{i=1}^{L} c_{i,\downarrow}^{\dagger} c_{i,\downarrow} = M, \tag{A.3}$$

where M and N are the numbers of the down spins and the electrons, respectively. We number each site consecutively from 1 to L. We here define the amplitude of the wave function Ψ as $\psi(x_1, x_2, \ldots, x_M | x_{M+1}, \ldots, x_N)$, where we put the down spins at $x_1, x_2, \ldots, x_M$ and the up spins at $x_{M+1}, \ldots, x_N$, respectively. Then we obtain the eigenvalue equation of (A.1) in the form

$$-t\sum_{i=1}^{L}\sum_{s=\pm 1}\psi(x_1,\ldots,x_i+s,\ldots,x_N)+U\sum_{i<j}\delta(x_i-x_j)\psi(x_1,\ldots,x_N)=E\psi(x_1,\ldots,x_N). \tag{A.4}$$

Now we consider the following ansatz for ψ, namely the Bethe-ansatz wave function:

$$\psi(x_1, x_2, \ldots, x_M | x_{M+1}, \ldots, x_N) = \sum_{P} [Q, P] \exp(i \sum_{j=1}^{N} k_{P_j} x_{Q_j}). \tag{A.5}$$

The symbol $P = (P_1, P_2, \ldots, P_N)$ and $Q = (Q_1, Q_2, \ldots, Q_N)$ are permutations of the numbers $(1, 2, \ldots, N)$ with $1 \leq x_{Q_1} \leq x_{Q_2} \leq \cdots \leq x_{Q_N} \leq L$. The symbol $[Q, P]$ is a set of $N! \times N!$ coefficients depending on the two permutations P and Q. The quasimomenta $k_1, k_2, \ldots, k_N$ are real and unequal to each other for the ground state. The coefficient $[Q, P]$ is related to the scattering matrices and produces the Bethe-ansatz equation.

A.2 The exact analysis of the Hubbard model

Let us first demonstrate the calculation of $[Q, P]$ for $L = 2, M = 1$ and $N = 2$. We make the following ansatz for ψ:

$$\begin{aligned}\psi(x_1, x_2) =& \theta(x_2 - x_1) \left([12, 12] e^{i(k_1 x_1 + k_2 x_2)} + [12, 21] e^{i(k_2 x_1 + k_1 x_2)} \right) \\ &+ \theta(x_1 - x_2) \left([21, 12] e^{i(k_2 x_1 + k_1 x_2)} + [21, 21] e^{i(k_2 x_1 + k_2 x_1)} \right), \end{aligned} \tag{A.6}$$

where $\theta(x_1 - x_2)$ is a step function in the form

$$\begin{aligned} \theta(x_1 - x_2) &= 1 \qquad x_1 > x_2, \\ \theta(x_1 - x_2) &= 0 \qquad x_2 > x_1. \end{aligned} \tag{A.7}$$

Equation (A.4) is rewritten in the form

$$\begin{aligned} &- t\psi(x_1 + 1, x_2) - t\psi(x_1 - 1, x_2) - t\psi(x_1, x_2 + 1) - t\psi(x_1, x_2 - 1) \\ &+ U\delta(x_2 - x_1)\psi(x_1, x_2) = E\psi(x_1, x_2). \end{aligned} \tag{A.8}$$

We substitute Eq. (A.6) for ψ in Eq. (A.8) and obtain the following three relations:

$$E = -2t(\cos k_1 + \cos k_2), \tag{A.9}$$

$$[12,12] + [12,21] - [21,12] - [21,21] = 0, \tag{A.10}$$

$$2ti(\sin k_1 - \sin k_2)([12,12] - [12,21] + [21,12] - [21,21]) + U([12,12] + [12,21]) = 0. \tag{A.11}$$

From Eqs. (A.10) and (A.11), we have

$$\begin{pmatrix}[12,21]\\[21,21]\end{pmatrix} = \frac{1}{\sin k_1 - \sin k_2 - iU/2t} \begin{pmatrix} -iU/2t & \sin k_1 - \sin k_2 \\ \sin k_1 - \sin k_2 & -iU/2t \end{pmatrix} \begin{pmatrix}[12,12]\\[21,12]\end{pmatrix}. \tag{A.12}$$

The relation

$$\begin{pmatrix}[12,12]\\[12,21]\end{pmatrix} = \begin{pmatrix}[21,12]\\[21,21]\end{pmatrix}, \tag{A.13}$$

should be satisfied since the wave function is symmetric

$$\psi(x_1, x_2) = \psi(x_2, x_1)$$

by the exchange of the two particles, one up spin and one down spin. We here introduce

$$\xi_{21} = \left[\frac{-iU/2t}{\sin k_1 - \sin k_2 + iU/2t} I + \frac{\sin k_1 - \sin k_2}{\sin k_1 - \sin k_2 + iU/2t} P_{12}\right] \xi_{12}, \tag{A.14}$$

where

$$\xi_{12} = \begin{pmatrix}[12,12]\\[21,12]\end{pmatrix}, \quad \xi_{21} = \begin{pmatrix}[12,21]\\[21,21]\end{pmatrix} \tag{A.15}$$

and I is the identity operator. The matrix P_{12} is a pair-exchange operator where $P_{12} = I$ in the singlet case (the present case) and $P_{12} = -I$ in the triplet case. We here define Y_{12}^{12} in the form

$$Y_{12}^{12} = \frac{-iU/2t}{\sin k_1 - \sin k_2 + iU/2t} I + \frac{\sin k_1 - \sin k_2}{\sin k_1 - \sin k_2 + iU/2t} P_{12}. \tag{A.16}$$

Hence we have

$$\xi_{21} = Y_{12}^{12} \xi_{12}. \tag{A.17}$$

We note that $Y_{12}^{12} Y_{21}^{12} = I$ is satisfied both for the singlet state and for the triplet state. The matrix Y is often called the scattering matrix.

For arbitrary L, M and N, Y_{ij}^{ab} is in the from [1]

$$Y_{ij}^{ab} = \frac{-iU/2t}{\sin k_i - \sin k_j + iU/2t} I + \frac{\sin k_i - \sin k_j}{\sin k_i - \sin k_j + iU/2t} P_{ab}, \tag{A.18}$$

where

$$\begin{aligned} &Q_n = a = Q'_{n+1}, \quad Q_{n+1} = b = Q'_n, \quad Q_l = Q'_l \quad \text{for } l \neq n, n+1, \\ &P_n = i = P'_{n+1}, \quad P_{n+1} = j = P'_n, \quad P_l = P'_l \quad \text{for } l \neq n, n+1, \end{aligned} \tag{A.19}$$

and P_{ab} is an operator which exchanges $Q_n = a$ and $Q_{n+1} = b$. Hence we reach the equation

$$[Q, P] = Y_{ij}^{ab}[Q', P']. \tag{A.20}$$

C. N. Yang derived the Bethe-ansatz equations from the scattering matrix Y_{ij}^{ab} in the continuum gas case [19]. Lieb and Wu applied this technique to the Hubbard model and derived the following equations by considering replacing k with $\sin k$ in the lattice gas [1]:

$$\begin{aligned} \exp(iLk_j) &= \prod_{\beta=1}^{M} \frac{\sin k_j - \Lambda_\beta + iU/4t}{\sin k_j - \Lambda_\beta - iU/4t} \qquad (j = 1, \ldots, N), \\ \prod_{j=1}^{N} \frac{\sin k_j - \Lambda_\alpha + iU/4t}{\sin k_j - \Lambda_\alpha - iU/4t} &= -\prod_{\beta=1}^{M} \frac{\Lambda_\alpha - \Lambda_\beta - iU/4t}{\Lambda_\alpha - \Lambda_\beta + iU/4t} \qquad (\alpha = 1, \ldots, M), \end{aligned} \tag{A.21}$$

where k and Λ are the rapidity of the charge and the spin, respectively. By taking the logarithm of Eq. (A.21), we have

$$\begin{aligned} Lk_j &= 2\pi I_j - 2\sum_{\beta=1}^{M} \arctan \frac{\sin k_j - \Lambda_\beta}{U/4t}, \\ \sum_{j=1}^{N} 2\arctan \frac{\Lambda_\alpha - \sin k_j}{U/4t} &= 2\pi J_\alpha + \sum_{\beta=1}^{M} 2\arctan \frac{\Lambda_\alpha - \Lambda_\beta}{U/2t}, \end{aligned} \tag{A.22}$$

where I_j and J_α are successive numbers centered around the origin for the ground state:

$$\begin{aligned} I_j &= \frac{N-1}{2}, \frac{N-3}{2}, \ldots, -\frac{N-1}{2}, \\ J_\alpha &= \frac{M-1}{2}, \frac{M-3}{2}, \ldots, -\frac{M-1}{2}. \end{aligned} \tag{A.23}$$

Now we put $N/L = 1$ and $M/L = 1/2$. We introduce $f(k_j) = I_j/L$ and $g(\Lambda_\alpha) = J_\alpha/L$ and we define the distribution functions of charge and the spin as $\rho(k_j) \equiv f'(k_j)$ and $\sigma(\Lambda) \equiv g'(\Lambda)$, respectively. We rewrite Eq. (A.22) in the form of Fredholm-type integral equations

$$\begin{aligned} k &= 2\pi f(k) - \int_{-B}^{B} 2\arctan \frac{\sin k - \Lambda}{U/4t} \sigma(\Lambda) d\Lambda, \\ \int_{-Q}^{Q} 2\arctan \frac{\Lambda - \sin k}{U/4t} \rho(k) dk &= 2\pi g(\Lambda) + \int_{-B}^{B} 2\arctan \frac{\Lambda - \Lambda'}{U/2t} \sigma(\Lambda') d\Lambda'. \end{aligned} \tag{A.24}$$

By differentiating Eq. (A.24) with respect to k and Λ, we have

$$\rho(k) = \frac{1}{2\pi} + \frac{\cos k}{\pi} \int_{-B}^{B} \frac{U/4t}{(U/4t)^2 + (\Lambda - \sin k)^2} \sigma(\Lambda) d\Lambda, \tag{A.25}$$

$$\sigma(\Lambda) = \frac{1}{\pi} \int_{-Q}^{Q} \frac{U/4t}{(U/4t)^2 + (\Lambda - \sin k)^2} \rho(k) dk - \frac{1}{\pi} \int_{-B}^{B} \frac{U/2t}{(U/2t)^2 + (\Lambda - \Lambda')^2} \sigma(\Lambda') d\Lambda'. \tag{A.26}$$

The integral ranges Q and B are determined in order to satisfy the following relation

$$\begin{aligned} \int_{-Q}^{Q} \rho(k) dk &= N/L = 1, \\ \int_{-B}^{B} \sigma(\Lambda) d\Lambda &= M/L = 1/2, \end{aligned} \tag{A.27}$$

where we have to set $Q = \pi$ and $B = \infty$ in the half-filled case.

We now solve the integral equations (A.25) and (A.26). We substitute Eq. (A.25) into Eq. (A.26) and obtain

$$\begin{aligned} \sigma(\Lambda) =& \frac{1}{2\pi^2} \int_{-\pi}^{\pi} \frac{U/4t}{(U/4t)^2 + (\Lambda - \sin k)^2} dk \\ & - \frac{1}{\pi^2} \int_{-\infty}^{\infty} \sigma(\Lambda) d\Lambda \int_{-\pi}^{\pi} \frac{(U/4t)^2}{\left((U/4t)^2 + (\Lambda - \sin k)^2\right)^2} d(\Lambda - \sin k) \\ & - \frac{1}{\pi} \int_{-\infty}^{\infty} \frac{U/2t}{(U/2t)^2 + (\Lambda - \Lambda')^2} \sigma(\Lambda') d\Lambda' \\ =& \frac{1}{2\pi^2} \int_{-\pi}^{\pi} \frac{U/4t}{(U/4t)^2 + (\Lambda - \sin k)^2} dk - \frac{1}{\pi} \int_{-\infty}^{\infty} \frac{U/2t}{(U/2t)^2 + (\Lambda - \Lambda')^2} \sigma(\Lambda') d\Lambda'. \end{aligned} \tag{A.28}$$

We can solve Eq. (A.28) by operating the Fourier transformation of $\sigma(\Lambda)$:

$$\begin{aligned} \tilde{\sigma}(\omega) =& \int_{-\infty}^{\infty} e^{-i\omega\Lambda} \sigma(\Lambda) d\Lambda \\ =& \underbrace{\frac{1}{2\pi^2} \int_{-\infty}^{\infty} e^{-i\omega\Lambda} d\Lambda \int_{-\pi}^{\pi} \frac{U/4t}{(U/4t)^2 + (\Lambda - \sin k)^2} dk}_{I_1} \\ & \underbrace{- \frac{1}{\pi} \int_{-\infty}^{\infty} e^{-i\omega\Lambda} d\Lambda \int_{-\infty}^{\infty} \frac{U/2t}{(U/2t)^2 + (\Lambda - \Lambda')^2} \sigma(\Lambda') d\Lambda'}_{I_2}, \end{aligned} \tag{A.29}$$

where

$$
\begin{aligned}
I_1 &= \frac{1}{2\pi^2}\frac{U}{4t}\int_{-\pi}^{\pi} dk e^{-i\omega\sin k}\underbrace{\int_{-\infty}^{\infty}\frac{e^{-i\omega\lambda}}{(U/4t)^2+\lambda^2}d\lambda}_{\frac{4\pi t}{U}e^{-\frac{U}{4t}|\omega|}} \quad (\lambda=\Lambda-\sin k)\\
&= \frac{1}{2\pi^2}\frac{U}{4t}\int_{-\pi}^{\pi} dk e^{-i\omega\sin k}\frac{4\pi t}{U}e^{-\frac{U}{4t}|\omega|}\\
&= \frac{1}{2\pi}e^{-\frac{U}{4t}|\omega|}\int_{-\pi}^{\pi} e^{-i\omega\sin k}dk,\\
I_2 &= -\frac{1}{\pi}\int_{-\infty}^{\infty}\frac{U}{2t}\sigma(\Lambda')e^{-i\omega\Lambda'}d\Lambda'\underbrace{\int_{-\infty}^{\infty}\frac{e^{-i\omega\lambda'}}{(U/2t)^2+\lambda'^2}d\lambda'}_{\frac{\pi}{U/2t}e^{-\frac{U}{2t}|\omega|}} \quad (\lambda'=\Lambda-\Lambda')\\
&= -\frac{1}{\pi}\int_{-\infty}^{\infty}\frac{U}{2t}\sigma(\Lambda')e^{-i\omega\Lambda'}d\Lambda'\frac{\pi}{U/2t}e^{-\frac{U}{2t}|\omega|}\\
&= -e^{-\frac{U}{2t}|\omega|}\int_{-\infty}^{\infty}\sigma(\Lambda')e^{-i\omega\Lambda'}d\Lambda'\\
&= -e^{-\frac{U}{2t}|\omega|}\tilde{\sigma}(\omega).
\end{aligned}
\tag{A.30}
$$

Hence we have

$$
\tilde{\sigma}(\omega) = \frac{1}{4\pi}\int_{-\pi}^{\pi}\mathrm{sech}\left(\frac{U}{4t}\omega\right)e^{i\omega\sin k}dk. \tag{A.31}
$$

We obtain $\sigma(\Lambda)$ by operating the inverse Fourier transformation of $\tilde{\sigma}(\omega)$:

$$
\begin{aligned}
\sigma(\Lambda) =& \frac{1}{2\pi}\int_{-\infty}^{\infty}\tilde{\sigma}(\omega)e^{-i\Lambda\omega}d\omega\\
=& \frac{1}{8\pi^2}\int_{-\infty}^{\infty}d\omega\mathrm{sech}\left(\frac{U}{4t}\omega\right)e^{-i\Lambda\omega}\underbrace{\int_{-\pi}^{\pi}e^{-i\omega\sin k}dk}_{2\pi J_0(\omega)}\\
=& \frac{1}{2\pi}\int_{0}^{\infty}\mathrm{sech}\left(\frac{U}{4t}\omega\right)\cos(\Lambda\omega)J_0(\omega)d\omega.
\end{aligned}
\tag{A.32}
$$

We obtain $\rho(k)$ by substituting $\sigma(\Lambda)$ into Eq. (A.25):

$$\begin{aligned}\rho(k) =&\frac{1}{2\pi}+\frac{\cos k}{\pi}\frac{1}{2\pi}\int_0^\infty d\omega \mathrm{sech}\left(\frac{U}{4t}\omega\right)J_0(\omega)\underbrace{\int_{-\infty}^{\infty}\cos(\Lambda\omega)\frac{U/4t}{(U/4t)^2+(\Lambda-\sin k)^2}d\Lambda}_{\cos(\omega\sin k)\int_{-\infty}^{\infty}\cos(\lambda\omega)\frac{U/4t}{(U/4t)^2+\lambda^2}d\lambda}\\ =&\frac{1}{2\pi}+\frac{1}{2\pi}\frac{\cos k}{\pi}\frac{U}{4t}\int_0^\infty d\omega \mathrm{sech}\left(\frac{U}{4t}\omega\right)J_0(\omega)\cos(\omega\sin k)\underbrace{\int_{-\infty}^{\infty}\cos(\lambda\omega)\frac{U/4t}{(U/4t)^2+\lambda^2}d\lambda}_{\frac{4\pi t}{U}e^{-\frac{U}{4t}\omega}}\\ =&\frac{1}{2\pi}+\frac{\cos k}{\pi}\int_0^\infty\frac{\cos(\omega\sin k)J_0(\omega)}{1+\exp(\omega U/2t)}d\omega. \qquad (A.33)\end{aligned}$$

The ground state energy per site is given by

$$\begin{aligned}E_{\rm gs} =&-2t\int_{-\pi}^{\pi}\cos k\rho(k)dk\\ =&-\frac{t}{\pi}\int_{-\pi}^{\pi}\cos k dk-\frac{2t}{\pi}\int_0^\infty d\omega\frac{J_0(\omega)}{1+e^{\omega U/2t}}\underbrace{\int_{-\pi}^{\pi}dk\cos^2 k\cos(\omega\sin k)}_{2\pi J_1(\omega)/\omega}\\ =&-4t\int_0^\infty\frac{J_0(\omega)J_1(\omega)}{\omega[1+\exp(\omega U/2t)]}d\omega. \qquad (A.34)\end{aligned}$$

A.3 Hubbard gap by the charge excitation

The energy gap due to the charge excitation exists for any finite U in the half-filled case. The one-hole excitation energy at $k_h=\pm\pi$ gives the Hubbard gap. We here calculate the Hubbard gap analytically.

The Hubbard gap is defined in terms of the chemical potential. We define the chemical potential μ_+ as we take one electron into the system and μ_- as we take one electron out. The chemical potential μ_+ and μ_- are given by

$$\begin{aligned}\mu_+ &= E(n_\uparrow+1,n_\downarrow)-E(n_\uparrow,n_\downarrow),\\ \mu_- &= E(n_\uparrow,n_\downarrow)-E(n_\uparrow-1,n_\downarrow), \qquad (A.35)\end{aligned}$$

where $n_\uparrow$ and $n_\downarrow$ are the numbers of the up spins and the down spins, respectively. Now consider the following transformations:

$$\begin{aligned}c^\dagger_{i,\uparrow}c^\dagger_{i,\downarrow}|\mathrm{vac}\rangle &\rightarrow |\mathrm{vac}\rangle,\\ c^\dagger_{i,\uparrow}|\mathrm{vac}\rangle &\rightarrow c^\dagger_{i,\downarrow}|\mathrm{vac}\rangle,\\ c^\dagger_{i,\downarrow}|\mathrm{vac}\rangle &\rightarrow c^\dagger_{i,\uparrow}|\mathrm{vac}\rangle,\\ |\mathrm{vac}\rangle &\rightarrow c^\dagger_{i,\uparrow}c^\dagger_{i,\downarrow}|\mathrm{vac}\rangle. \qquad (A.36)\end{aligned}$$

The energy difference ΔE due to the transformations is

$$\Delta E = E(L - n_\uparrow, L - n_\downarrow) - E(n_\uparrow, n_\downarrow) = (n_{\text{double}} - n_{\text{vac}})U, \tag{A.37}$$

where n_{double} and n_{vac} are the number of double occupancies and the number of the vacuum states, respectively. The following relation is satisfied because the summation of the numbers of the vacuum state, the up-spin state, the down-spin state and the full state is L:

$$n_{\text{vac}} + (n_\uparrow - n_{\text{double}}) + (n_\downarrow - n_{\text{double}}) + n_{\text{double}} = L. \tag{A.38}$$

Hence we have

$$n_{\text{vac}} - n_{\text{double}} = L - n_\uparrow - n_\downarrow. \tag{A.39}$$

Substituting Eq. (A.39) into Eq. (A.37),

$$\Delta E = E(L - n_\uparrow, L - n_\downarrow) - E(n_\uparrow, n_\downarrow) = (L - n_\uparrow - n_\downarrow)U. \tag{A.40}$$

The definition of the Hubbard gap is given by

$$\Delta = \mu_+ - \mu_-. \tag{A.41}$$

In the half-filled case, that is, $n_\uparrow = n_\downarrow = M(= L/2)$, we rewrite μ_+ as following

$$\begin{aligned}\mu_+ =& E(M+1, M) - E(M, M) \\ =& E(L-(M+1), L-M) - [L-(M+1)-M]U - E(M, M) \\ =& E(M-1, M) - E(M, M) + U = -\mu_- + U.\end{aligned} \tag{A.42}$$

Hence we can rewrite the Hubbard gap as follows:

$$\Delta = U - 2\mu_-. \tag{A.43}$$

For the calculation of μ_-, we remove an electron whose quasimomentum is k_h. The distribution of I_j changes into

$$I_j = \frac{N-1}{2}, \ldots, \frac{N-2h+3}{2}, \ldots, \frac{N-2h-1}{2}, \ldots, -\frac{N-1}{2}, \tag{A.44}$$

where we remove the $(h-1)$th quantum number. Referring to Eqs. (A.25) and (A.26), we obtain the following equations:

$$\begin{aligned}\rho(k) &= \frac{1}{2\pi} - \frac{1}{L}\delta(k - k_h) + \frac{\cos k}{\pi}\int_{-\infty}^{\infty} \frac{U/4t}{(U/4t)^2 + (\Lambda - \sin k)^2}\sigma(\Lambda)d\Lambda, \\ \sigma(\Lambda) &= \frac{1}{\pi}\int_{-\pi}^{\pi} \frac{U/4t}{(U/4t)^2 + (\Lambda - \sin k)^2}\rho(k)dk - \frac{1}{\pi}\int_{-\infty}^{\infty} \frac{U/2t}{(U/2t)^2 + (\Lambda - \Lambda')^2}\sigma(\Lambda')d\Lambda',\end{aligned} \tag{A.45}$$

where the distribution function $\rho_{\rm gs}(k)$ for the ground state changes into $\rho_{\rm gs}(k) - \frac{1}{L}\delta(k-k_h)$ by the one-hole excitation at $k = k_h$. The solution of Eq. (A.45) is given by

$$\begin{aligned}\sigma(\Lambda) =& \frac{1}{\pi}\int_0^\infty \mathrm{sech}\left(\frac{U}{4t}\omega\right)\cos(\Lambda\omega)J_0(\omega)d\omega \\ & - \frac{t}{4UL}\mathrm{sech}\left[\frac{2\pi t}{U}(\Lambda - \sin k_h)\right], \\ \rho(k) =& \frac{1}{2\pi} + \frac{\cos k}{\pi}\int_0^\infty \frac{\cos(\omega\sin k)J_0(\omega)}{1+\exp(U\omega/2t)} - \frac{1}{L}\delta(k-k_h) \\ & - \frac{1}{\pi L}\int_0^\infty \frac{d\omega}{1+\exp(U\omega/2t)}\int_{-\pi}^{\pi}\cos^2 k\cos\omega(\sin k - \sin k_h)dk. \end{aligned} \tag{A.46}$$

We define the shift of $\rho(k)$ as

$$\Delta\rho(k) = -\frac{1}{L}\delta(k-k_h) - \frac{1}{\pi L}\int_0^\infty \frac{d\omega}{1+\exp(U\omega/2t)}\int_{-\pi}^{\pi}\cos^2 k\cos[\omega(\sin k - \sin k_h)]dk. \tag{A.47}$$

We obtain the excitation energy $\varepsilon(k_h)$ at $k = k_h$ as

$$\varepsilon(k_h) = -2t\int_{-\pi}^{\pi}\cos k\Delta\rho(k)dk. \tag{A.48}$$

The lowest energy gap at $k_h = \pm\pi$ gives the Hubbard gap. The excitation energy $\varepsilon(k_h = \pm\pi)$ is given by

$$\begin{aligned}\varepsilon(k_h = \pm\pi) =& -2t\left[-1 + \frac{1}{\pi}\int_0^\infty \frac{d\omega}{1+\exp(U\omega/2t)}\int_{-\pi}^{\pi}\cos^2 k\cos(\omega\sin k)dk\right] \\ =& -2t\left[-1 + 2\int_0^\infty \frac{J_1(\omega)d\omega}{\omega(1+\exp(U\omega/2t))}\right]. \end{aligned} \tag{A.49}$$

Hence we obtain the Hubbard gap

$$\begin{aligned}\Delta =& U - 2\mu_- \\ =& U - 4t\left[1 - 2\int_0^\infty \frac{J_1(\omega)d\omega}{\omega(1+\exp(U\omega/2t))}\right]. \end{aligned} \tag{A.50}$$

Figure A.1 shows the Hubbard gap Δ as a function of U. We note that the Hubbard gap exists for any finite U.

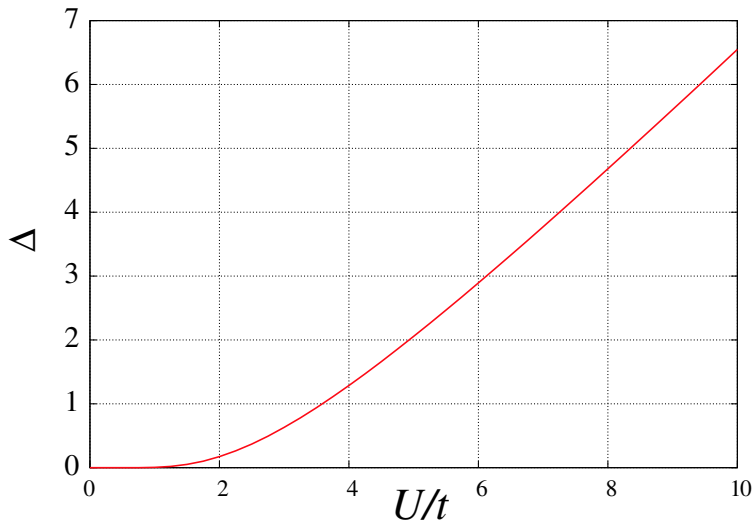

Figure A.1: The U dependence of the Hubbard gap Δ.

Bibliography

[1] E. H. Lieb and F. Y. Wu, Phys. Rev. Lett. **20** (1968) 1445

[2] C. A. Stafford and A. J. Millis, Phys. Rev. B **48** (1993) 1409

[3] Y. Umeno and M. Shiroishi, Euro. Phys. Lett. **62** (2003) 384

[4] Z. Hiroi, M. Azuma, M. Takano and Y. Bando, J. Solid State Chem. **95** (1991) 230

[5] M. C. Gutzwiller, Phys. rev. Lett. **10** (1963) 159; Phys. Rev. **134A** (1964) 923; ibid. 137A (1965) 1726

[6] H. Yokoyama and H. Shiba, J. Phys. Soc. Jpn. **56** (1986) 1490

[7] N. Hatano and D. R. Nelson, Phys. Rev. Lett. **77** (1996) 570; Phys. Rev. B **56** (1997) 8651

[8] T. Fukui and N. Kawakami, Phys. Rev. B **58** (1998) 16051

[9] G. Albertini, S. R. Dahmen and B. Wehefritz, Nucl. Phys. B **493** (1997) 541

[10] R. M. Noack, S. R. White, and D. J. Scalapino, Phys. Rev. Lett. **73** (1994) 882; Physica C **270** (1996) 281

[11] H. Tsunetsugu, M. Sigrist, and K. Ueda, Rev. Mod. Phys. **69** (1997) 809

[12] C. N. Yang and C. P. Yang, Phys. Rev. **150** (1966) 321

[13] N. Hatano, unpublished

[14] J. D. Johnson, S. Krinsky, B. M. McCoy, Phys. Rev. A **8**, 2526 (1973)

[15] S. J. Gu, V. M. Pereira and N. M. R. Peres, Phys. Rev. B **66** (2002) 235108

[16] N. Hatano and Y. Nishiyama, J. Phys. A: Math. Gen. **28** (1995) 3911

[17] H. A. Bethe, Z. Physik **71** (1931) 205

[18] A. M. Tsvelisk and P. B. Wiegmann, Ad. Phys. **32** (1983) 453; N. Kawakami and A. Okiji, Phys. Lett. **86A** (1981) 483; A. Okiji and N. Kawakami, J. Appl. Phys. **55** (1984) 1931

[19] C. N. Yang, Phys. Rev. Lett. **19** (1967) 1312